

Project Number: ME-RLN-1105

# **Modeling the NorEaster Engine**

A Major Qualifying Project Report

Submitted to the Faculty

of the

WORCESTER POLYTECHNIC INSTITUTE

in partial fulfillment of the requirements for the

Degree of Bachelor of Science

in Mechanical Engineering

by

---

Malena Lund

---

Daniel Mullen

---

Matthew Rosen

---

Daniel Sullivan

April 26, 2012

Approved:

---

Prof. Robert Norton

---

Prof. John Hall

## Abstract

The United States Military has increased their demand for engines that can fly in Unmanned Aerial Vehicles (UAVs). These engines must be powerful and light enough to maximize the aircraft's efficiency. The objective of this project is to model the dynamic behavior of the O'Neill Motor Company, Inc.'s innovative coaxial counter-rotating cam engine called the NorEaster engine. The engine's output power was calculated using a mathematical model that we developed using Mathcad, and the weights of the newest NorEaster engine designs were obtained from another MQP team. Therefore, we were able to calculate the power to weight ratio of the NorEaster engine. The military's desired minimum power to weight ratio for the NorEaster engine is 0.5. Additionally, we performed dynamometer tests and pressure tests on the existing NorEaster engine prototype and developed mathematical models for both gasoline and diesel NorEaster engine designs. A future NorEaster engine that operates on gasoline, has a 4 inch bore, a firing temperature of 2000 K, and a compression ratio of 10 is predicted to have a power to weight ratio of 0.46. Similarly, a future NorEaster engine design that operates on diesel fuel with a 4 inch bore, a cut off ratio of 2.75, and a compression ratio of 20 is predicted to have a power to weight ratio of 0.49. Based on these results, we recommend further development of an eight cylinder diesel engine with the specified parameters.

## Executive Summary

The NorEaster engine designed by the O'Neill Motor Company, Inc. is an innovative cam engine that utilizes coaxial counter rotation to generate lift for Unmanned Aerial Vehicles (UAVs). The objective of this report is to calculate the power to weight ratio of the NorEaster engine and the new designs associated with it. The military's desired minimum power to weight ratio for the NorEaster engine is 0.5.

## Methodology

In order to understand the strengths and weaknesses of the existing NorEaster prototype, we researched the types of rotors used on helicopters and performed dynamometer and pressure tests on the current prototype engine.

During our rotor analysis, we assessed the limitations on the diameter of the rotor blades and learned how they vary with angular velocity. To ensure a safe and reliable flight, the rotor tip velocity must remain subsonic. Given this limitation, we discovered that the maximum rotor radius varies with altitude, forward speed and rpm. The maximum engine rpm values are 3120, 4052, and 4984 for the three forward speeds of 300 mph, 200 mph and 100 mph, respectively. We discovered that the engine will stall at an angle of attack of approximately 20 degrees when using the requested airfoil, NACA 0015.

In addition to rotor analysis, we analyzed the output power of the existing NorEaster engine by performing a dynamometer test. We calculated the power of the prototype engine by measuring the current and voltage across several resistors. From this test, we discovered that the output power increased by 0.389 horsepower for every increase of 100 rpm. As anticipated, the power produced by the prototype NorEaster engine increased as the engine's rpm increased.

Finally, we performed a pressure test to calculate the pressure inside the cylinders of the prototype NorEaster engine. We installed a Dytran pressure transducer on the inside surface of the cylinder head and relayed its signal through a charge amplifier. We read the signal on an HP Dynamic Signal Analyzer in mV as a function of time and converted it to psi using a 6.22 mV/psi conversion factor that we measured during a calibration test. During the pressure test, we mounted a shaft encoder on the outer rotating shaft of the NorEaster engine in order to

pinpoint the piston's location at top dead center (TDC) in relation to the pressure readings. From this data, we discovered that there are some leaks in the current prototype, since its average maximum pressure reading was only 355.8 psi. Ideally, the maximum pressure inside of the cylinder head should be around 1000 psi.

## **Results**

Upon analyzing the prototype of the NorEaster engine, we decided to use the air-standard Otto Cycle analysis method to calculate the power produced by existing and future engine designs. We developed two mathematical models that calculate the anticipated power for the engine and divided it by the anticipated engine weight for diesel and gasoline designs. The values for the engine weight were determined by another MQP team that is working on designing a new NorEaster engine. For the gasoline engine, we recommend using a 4 inch bore with a compression ratio of 10 and a firing temperature of 2000 K in order to obtain a power to weight ratio of 0.46. For the diesel engine, we recommend using a 4 inch bore with a compression ratio of 20 and a cut-off ratio of 2.75 in order to obtain a power to weight ratio of 0.49.

## **Conclusion and Recommendations**

Based on the power to weight ratios that we calculated using our mathematical model, further development of the diesel NorEaster engine design is recommended. We would suggest building a second generation prototype of the NorEaster engine with eight cylinder heads and the optimized parameters provided above.

## Table of Contents

Abstract .....	i
Executive Summary .....	ii
List of Figures .....	vi
List of Tables .....	viii
1.0 Introduction.....	1
2.0 Literature Review.....	3
2.1 How an Engine Works .....	3
2.1.1 Four-Stroke Cycle.....	3
2.1.2 Isentropic Relationships .....	4
2.1.3 Air-Standard Otto Cycle Analysis .....	6
2.1.4 Crankshaft Engines.....	10
2.1.5 Cam Engines.....	11
2.1.6 The Existing NorEaster Engine Design.....	12
2.1.7 Engine Design Optimization .....	15
2.2 Comparison to Existing Drone Engines and Companies .....	15
3.0 Methodology .....	17
3.1 Free Body Diagram of the NorEaster Engine .....	17
3.2 Weight Calculations .....	18
3.3 Cylinder Compression Ratio Measurement .....	19
3.4 Mechanical Compression Test .....	20
3.5 Blade to Engine Relationships .....	20
3.5.1 Maximum Blade Diameter Compared to Engine RPM.....	20
3.5.2 Limitations of NACA0015 .....	21
3.6 Dynamometer Testing .....	24

3.6.1 Procedure .....	24
3.6.2 Dynamometer Test 1 Results.....	25
3.6.3 Dynamometer Test 2 Results.....	27
3.7 Pressure Transducer Test .....	28
3.7.1 Procedure .....	28
3.7.2 Pressure Transducer Test Results .....	31
4.0 Results.....	37
4.1 Gasoline Engine Results.....	37
4.1.1 Current Gasoline Engine Results.....	41
4.2 Diesel Engine Results.....	41
4.3 Overall Findings for the NorEaster Engine Designs.....	43
5.0 Conclusions and Recommendations .....	45
6.0 References.....	47
Appendix A – Blade to Engine Relationships .....	50
Appendix B – Dynamometer Mathcad .....	51
Appendix C – Gasoline and Diesel Mathematical Models.....	55
Gasoline Engine Model.....	55
Diesel Engine Model.....	63

## List of Figures

Figure 1: Pressure versus Volume Diagram for an Ideal Otto Cycle (Glenn Research Center, 2008) .....	4
Figure 2: Given Parameters and Variables from a Sample Problem (Moran and Shapiro, 2011)..	8
Figure 3: Increase in Power as the Engine Speed Increases .....	9
Figure 4: Pressure versus Volume Diagram of an Actual Otto Cycle (MIT, 2006) .....	9
Figure 5: Thermal Efficiency depending on the Compression Ratio (MIT, 2006) .....	10
Figure 6: The Interior of a V-Arrangement Crank Shaft Engine (Loeffler, 2003) .....	11
Figure 7: The NorEaster Engine's Two-Lobe Cam Design.....	12
Figure 8: The NorEaster's Existing Cam Design .....	13
Figure 9: View of the Snowflake Plate Inside of the NorEaster Engine .....	14
Figure 10: Fully Assembled NorEaster Engine .....	14
Figure 11: The Sikorsky X2.....	16
Figure 12: Free Body Diagram of the NorEaster Engine .....	17
Figure 13: Graph of the Propeller Blade Diameter vs. the Potential Revolutions per Minute .....	21
Figure 14: Image of the NACA 0015 Providing Lift and Drag Coefficients (MIT XFOIL).....	22
Figure 15: Lift and Drag Coefficients of NACA 0015 at Varying Angles of Attack (CSEE) .....	23
Figure 16: Circuit Board Used for the Dynamometer Test Performed on the NorEaster Engine	25
Figure 17: Graph Comparing Horsepower to RPM.....	26
Figure 18: Graph Comparing Horsepower to RPM.....	28
Figure 19: PCB Charge Amplifier Model 462S05 .....	29
Figure 20: HP Signal Analyzer .....	29
Figure 21: The Valve and Gage Used to Calibrate the Pressure Transducer.....	30
Figure 22: Shaft Encoder Model 776 Mounted on the NorEaster Engine .....	31
Figure 23: Pressure Data: Compression Test.....	32
Figure 24: Pressure Data: Retarded Spark with Low Time Resolution.....	33
Figure 25: Pressure Data: Advanced Spark with High Time Resolution .....	34
Figure 26: Calibration Turning Force .....	35
Figure 27: Calibration Torque .....	35
Figure 28: Power to Weight Ratio as a Function of Firing Temperature .....	37

Figure 29: Power to Weight Ratio as a Function of Compression Ratio.....	38
Figure 30: Power to Weight Ratio as a Function of Bore Size.....	39
Figure 31: Equation to Calculate Weight as a Function of Bore Size .....	40
Figure 32: A 2 dimensional cross-section of a cylinder .....	40
Figure 33: Power to Weight Ratio as a Function of Cut-Off Ratio .....	41
Figure 34: Power to Weight Ratio as a Function of Compression Ratio.....	42
Figure 35: Power to Weight Ratio as a Function of Bore Size.....	42



## List of Tables

Table 1: Variables and Values Used to Calculate Power in Figure 2.....	7
Table 2: Current Two Cylinder Engine Component Weights .....	18
Table 3: Weights from the NorEaster Design Group’s SolidWorks Models.....	19
Table 4: Measurements to Calculate the Volume when the Piston is at Top Dead Center .....	19
Table 5: Comparison of RPM with Corresponding Horsepower.....	26
Table 6: Comparison of RPM with Corresponding Horsepower.....	27
Table 7: Pressure, Turning Force, and Torque Summation .....	36
Table 8: Comparison of the Power to Weight Ratios at Different Weight and Engine Parameters .....	43
Table 9: Fire Scout Power to Weight.....	44

## 1.0 Introduction

At the start of the 21<sup>st</sup> century, the United States military increased production of unmanned aerial vehicles (UAV). UAVs, also known as drones, are primarily used for two purposes: combat missions and surveillance missions. They minimize the harm presented to American troops and increase tactical advantages during war. Drones equipped with modern video and infrared technology can be used for surveillance missions. They can provide military officials with real-time images of dangerous locations that are of higher quality than the satellite images military officials currently rely on. Because UAVs are relatively small targets that are difficult to detect, they provide the military with new opportunities during war without putting soldiers in danger. Most UAVs are small airplanes that can quickly fly over an area and collect the information needed.

The military has recently developed a need for a more agile UAV that can provide clearer images and more accurate calculations for combat missions. Helicopter drones are an excellent way to meet this need since they can hover over an area for a period of time and easily move in all three dimensions. Upon recognizing this need, the O'Neill Motor Company, Inc. began developing a small cam engine that is intended for military helicopter drones. The NorEaster engine produces counter-rotation between two co-axial blades to obtain lift and thrust, so there is no need for a tail rotor. Due to the nature of this design, the most significant advantage of the engine is the inherent 4:1 gear reduction ratio that allows for slow revolutions of the shaft and eliminates the need for a gearbox.

The goal of our project is to identify the output power of the NorEaster engine in order to assess its uses in the field. The military's desired minimum power to weight ratio for the NorEaster engine is 0.5. We have concentrated our efforts on determining the output power of the NorEaster engine and identifying several parameters that can be adjusted in order to maximize it. The O'Neill Motor Company, Inc.'s objective is to design a NorEaster engine that meets the military's requirements and can be used to increase their capabilities.

Our project bridges the gap in information between the prototype design of the NorEaster engine and the development of a more effective product by creating a model which simulates the engine's performance. We researched means of optimizing an engine's power and identified the important aspects of engine design that must be considered in next generation engines. During

our investigation of the engine's output power, we compared our results to those of existing helicopter's to assess the benefits of the NorEaster engine.

In order to analyze the output power of the NorEaster engine, we modeled the engine in a computer program called Mathcad. Our mathematical model incorporates the thermodynamic equations for work and power of a four-stroke engine. We performed several power-related experiments to gather information on the NorEaster engine and assess the current design. These experiments and models were used to determine how to increase the engine's output power. Chapter 4 provides details on how to calculate the output power of the NorEaster engine and compares this innovative design to other competitive engine designs. The analysis of the information that we gathered led to the development of improved engine designs that can enhance the performance of the NorEaster engine and increase its appeal amongst the branches of the United States military that use UAV technology.

## 2.0 Literature Review

Aircraft engines have a variety of complicated and innovative designs. For example, fixed wing aircraft are typically propelled by turbofan engines, while rotating blade aircraft are often propelled by turboprop or turboshaft engines. The O'Neill Motor Company, Inc. has introduced another type of aircraft engine: the cam engine. The NorEaster engine uses a cam design to generate power.

### 2.1 How an Engine Works

Engines are machines containing moving parts that are used to generate motion. There are many different engine parameters, such as fuel type, compression ratio and bore size, that can be altered to accommodate different applications such as size, power, and weight. As each engine is designed to meet the desired specifications, these parameters can be modified to optimize the engine's performance for that application.

#### 2.1.1 Four-Stroke Cycle

The majority of gasoline powered reciprocating aircraft and vehicle engines operate on a four-stroke cycle called the Otto or Diesel cycle. As demonstrated in Figure 1, the four-stroke cycle goes through intake, compression, power, and exhaust strokes. The intake stroke begins with the piston positioned at top-dead center (TDC) and ends with the piston positioned at bottom-dead center (BDC), where the cylinder volume is at its maximum (stages A to 1). During this stroke, a fuel mixture is drawn into the cylinder through an inlet valve as the volume within the cylinder increases. As the inlet valve closes, the compression stroke is initiated. During this stroke (stages 1 to 2), the mixture within the cylinder is compressed and the piston slides to TDC again. Following the compression stroke, the pressure in the cylinder rapidly increases as the compressed fuel is ignited (stages 2 to 3). Next, the power stroke occurs as ignited fuel is converted into energy (stages 3 to 4). The exhaust valve is then opened (stages 4 to B). The exhaust stroke occurs as the piston reaches BDC and the gases and unburned mixture exit the cylinder (stages B to A).

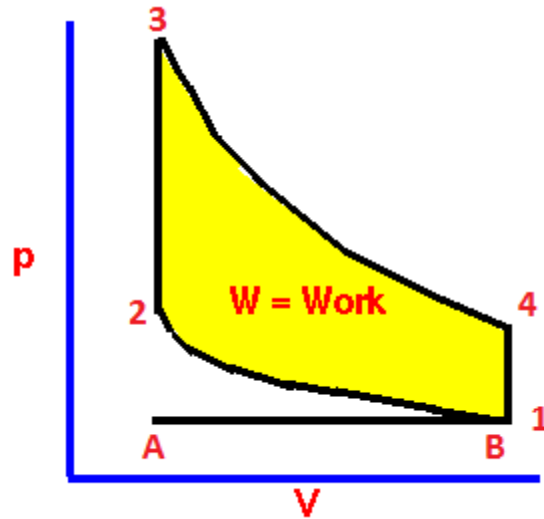


Figure 1: Pressure versus Volume Diagram for an Ideal Otto Cycle (Glenn Research Center, 2008)

As shown in Figure 1, each stage of the Otto Cycle varies depending on the pressure and the specific volume in an engine's cylinder head. The work is a function of the engine's pressures and compression ratio. The work per cycle is the area between the compression stroke and power stroke. Isentropic relationships can be used to assess the work, which is shaded in Figure 1. Upon analyzing the pressures and compression ratios at each of the different stages of the Otto cycle, the work and the power of a four-stroke engine can be determined.

### 2.1.2 Isentropic Relationships

When assessing the output work of an Otto Cycle, an isentropic relationship can be assumed for the compression and the power strokes. In an isentropic relationship, there is constant entropy; therefore, the process is both adiabatic and reversible (Moran, 2011, p. 315). The combination of these properties allow for engineers to use the Ideal Gas Tables to determine the relationship between the pressure, temperature, entropy, and internal energy at two different states. Therefore, the change in pressure,  $P$ , and temperature,  $T$ , can be determined by using the following equations,

$$\frac{P_2}{P_1} = r^\gamma$$

$$\frac{T_2}{T_1} = r^{1-\gamma}$$

where the compression ratio,  $r$ , is the ratio of maximum to minimum volume during the compression stroke and  $\gamma$  is the ratio of specific heats. During the combustion process (stages 2-3), heat is released by,

$$T_3 = T_2 + \frac{fQ}{C_v}$$

where  $Q$  is the heat released per pound of fuel, and  $f$  is the fuel to air ratio for combustion. Also the pressure during combustion,

$$P_3 = P_2 \left( \frac{T_3}{T_2} \right)$$

can be calculated from the ideal gas law. During the power stroke (stages 3-4), work is done on the piston by the gas. Equations used during the compression stroke can be used similarly to analyze both pressure and temperature during the expansion stroke. The relations used are:

$$\frac{P_4}{P_3} = r^{-\gamma}$$

$$\frac{T_4}{T_3} = r^{\gamma-1}$$

All heat is transferred to the surroundings between stages 4 and B in Figure 1; therefore, the temperature and pressure return to atmospheric conditions.

In a diesel engine, another parameter called the cut-off ratio,  $r_c$ , must be used to calculate the engine's output power. The cut-off ratio is the ratio of the volume in the cylinder at the start of ignition to the volume at the end of ignition (Engineering Software).

$$r_c = \frac{V_3}{V_2}$$

Work is done by the piston on the gas during the compression stroke and work is done by the gas on the piston during the expansion stroke. The difference between the work done during these two strokes is the work produced during the four-stroke cycle. Therefore the work,  $W$ , can be evaluated by the difference of the heat into the gas and the heat rejected by the gas which is represented by the formula:

$$W = C_v [(T_3 - T_2) - (T_4 - T_1)]$$

The output power of the engine is determined by dividing the work by the time it takes for one cycle to be completed.

### 2.1.3 Air-Standard Otto Cycle Analysis

An air-standard analysis is used when the temperature variation between several of the states exceeds 1000 K (Moran 2011, p 497). According to calculations performed in Chapter 4 of this report, the temperature in the existing NorEaster engine varies from room temperature (298 K) to over 1000 K, so the air-standard Otto Cycle analysis should be used to calculate the work.

During this cycle, one must assume that heat addition occurs instantaneously while the piston is at top dead center (Moran 2011, p 497). This causes the specific heat at constant pressure or constant volume to vary too much for the power calculation to depend on a constant value. Therefore, the work performed by the engine is calculated using internal energies at each of the four stages.

Figure 2 demonstrates how to use an air-standard analysis for an Otto Cycle based on an example from page 499-501 of Moran and Shapiro's "Fundamentals of Engineering Thermodynamics." Table 1 identifies the variables and known parameters for this example. The procedure used to calculate the power in this sample problem is also used to calculate the power of the NorEaster engine.

Title	Variable	Value
Specific Heat at Constant Volume	$C_v$	$53.3 \frac{ft * lbf}{lbm * R}$
Specific Heat Ratio	$\gamma$	1.4
Specific Gas Constant	$R_1$	$\frac{1545 ft * lbf}{28.97 lbm * R}$
Temperature at 2	$T_2$	540 R
Temperature at 3	$T_3$	3600 R
Temperature at 4	$T_4$	1878 R
Pressure	$P_2$	$14.696 \frac{lbf}{in^2}$
Volume	$V_2$	$0.02 ft^3$
Fuel Heating Value	$Q$	0.7 BTU
Compression Ratio	$r$	8
Cycle Frequency	$f_c$	1500 rpm
Ratio of Specific Volume at 2	$v_{r2}$	144.32
Ratio of Specific Volume at 4	$v_{r4}$	0.6449
Work	$W$	Calculated
Power	$H_p$	Calculated

Table 1: Variables and Values Used to Calculate Power in Figure 2



### Example

$$v_{r3} := V_r \cdot v_{r2} \quad v_{r5} := \frac{1}{V_r} v_{r4}$$

$$v_{r3} = 18.04 \quad v_{r5} = 5.159$$

$$\dot{m} := \frac{V_2 \cdot P_2}{R_1 \cdot T_2}$$

$$m = 1.47 \times 10^{-3} \text{ lb}$$

Alternate Method of finding T and u:

From T(2) and T(4) can find u values in Table A-22E

$$u_2 := 92.04 \frac{\text{BTU}}{\text{lb}} \quad u_4 := 721.44 \frac{\text{BTU}}{\text{lb}}$$

Put  $v(r3)$  into Table A-22E to get T(3) and T(5)

$$T_3 := 1212\text{R} \quad T_5 := 1878\text{R}$$

$$u_3 := 211.3 \frac{\text{BTU}}{\text{lb}} \quad u_5 := 342.2 \frac{\text{BTU}}{\text{lb}}$$

$$\dot{W} := m \cdot (u_4 - u_5 - u_3 + u_2)$$

$$\dot{W} = 0.382 \text{ BTU}$$

$$\dot{W} \cdot 1500 \text{ rpm} = 84.916 \text{ hp}$$

Figure 2: Given Parameters and Variables from a Sample Problem (Moran and Shapiro, 2011)

The graph in Figure 3 shows the theoretical engine speed versus the power that one cylinder outputs. It is based on the results of the power calculation performed in Figure 2. As can be viewed in the graph, power is directly related to speed. The slope of the line is 0.0566. This slope describes the rate at which the power increases with speed.

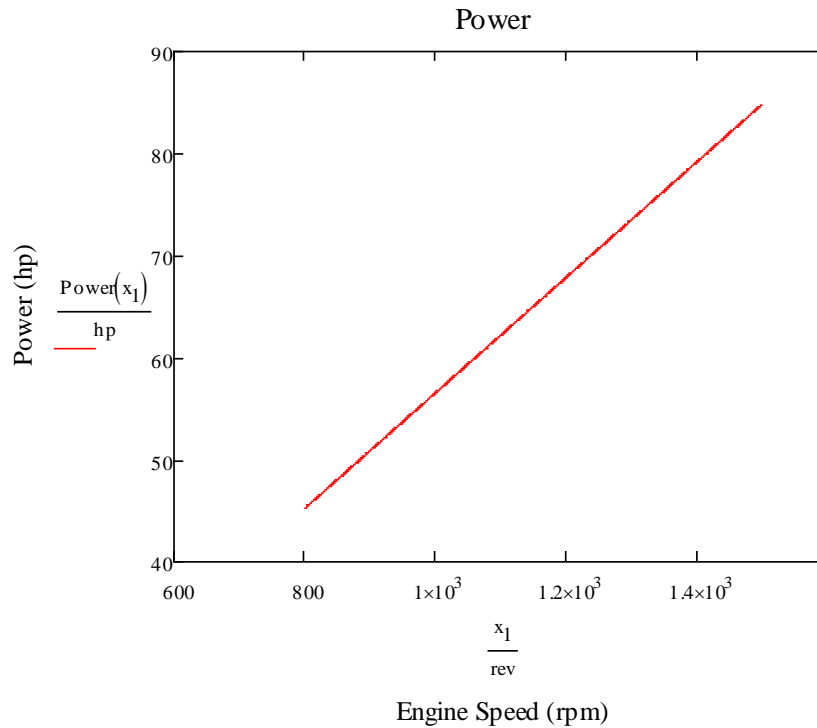


Figure 3: Increase in Power as the Engine Speed Increases

The final critical component of completing a power analysis for an Otto Cycle is the efficiency ( $\eta$ ). As demonstrated in Figure 4, an actual Otto Cycle does not follow the same pressure-volume curve as the ideal Otto Cycle does.

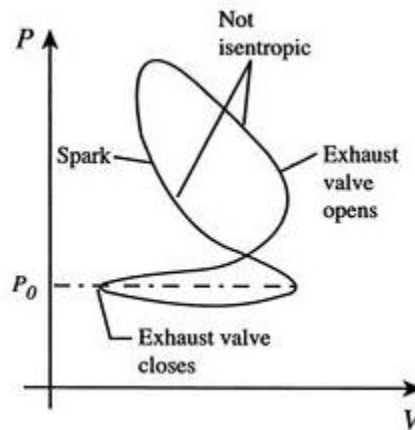


Figure 4: Pressure versus Volume Diagram of an Actual Otto Cycle (MIT, 2006)

In order to account for inefficiencies in an internal combustion engine, the value for  $\eta$  must be calculated using the following equation:

$$\eta = 1 + \frac{Q_{out}}{Q_{in}} = 1 - \frac{u_4 - u_1}{u_3 - u_2}$$

The actual output work is the product of the ideal output work and the efficiency rate. Modern internal combustion engines that use gasoline still have relatively low efficiencies compared to other methods of power generation such as turbines. However, turbines are too complex and expensive to completely replace the internal combustion engine.

For internal combustion engines, a correlation can be made between an engine's compression ratio and its efficiency. Figure 5 shows the typical engine efficiency for a gasoline fueled engine at various compression ratios.

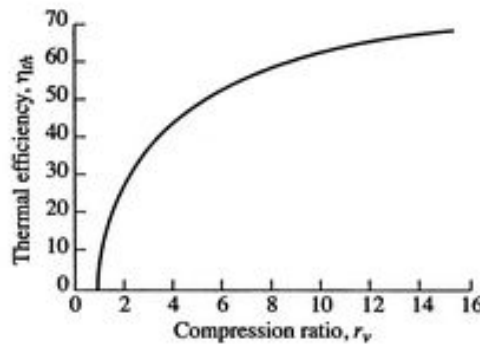


Figure 5: Thermal Efficiency depending on the Compression Ratio (MIT, 2006)

For an internal combustion engine with a compression ratio of 7, the ideal thermal efficiency is approximately 50% (MIT, 2006). However, the actual efficiency for an internal combustion engine averages only 30% (MIT, 2006). Since gasoline engines do not operate at their ideal state, the efficiency decreases by approximately 20%. As the compression ratio increases, the thermal efficiency of an internal combustion engine also increases, until it eventually approaches a maximum efficiency.

### 2.1.4 Crankshaft Engines

Crankshaft engines consist of pistons that reciprocate within cylinders and transmit power to a crankshaft through a connecting rod. The connecting rods are attached to the crankshaft and oscillate around the shaft while the pistons move within the cylinder. The cylinders of the engine are typically arranged in one of three ways: inline, V, or flat. When arranged inline, all cylinders are aligned in a single bank. Both V arrangements (Figure 6) and

flat arrangements consist of cylinders arranged in two banks in which the cylinders are set at an angle to one another or with the angle being 180 degrees for an approved engine.

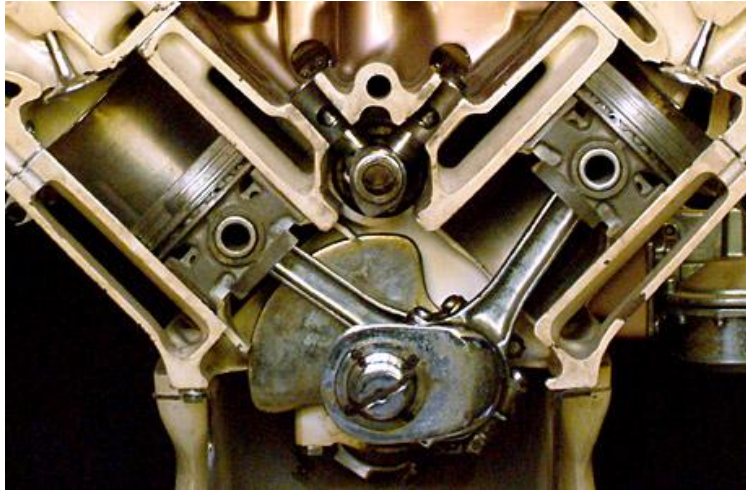
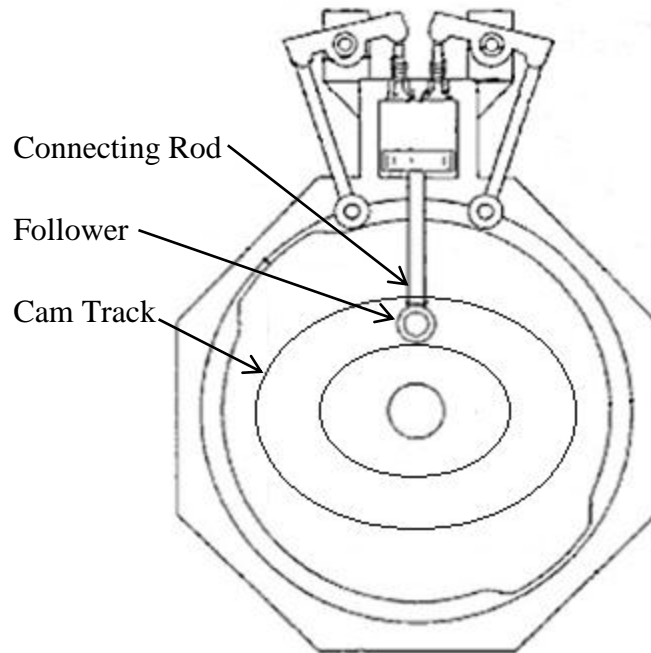


Figure 6: The Interior of a V-Arrangement Crank Shaft Engine (Loeffler, 2003)

### 2.1.5 Cam Engines

Similar to crankshaft engines, cam engines also consist of a piston that reciprocates within cylinders powered by a two- or four-stroke combustion process. The difference is that the connecting rods motion is strictly translational. This restricts pivoting at the linkage between the piston and the connecting rod. Consequently, the connecting rods do not rotate around a crankshaft. Instead, the connecting rods have followers which move within the groove of a rotating cam, as shown in Figure 7. A four lobe cam allows the pistons to complete two 4-stroke cycles while the cam only revolves once. This internal gearless reduction produces high torque and low rpm. A helicopter can use a cam engine to increase the output power since there is no gearbox.



**Figure 7: The NorEaster Engine's Two-Lobe Cam Design**

### **2.1.6 The Existing NorEaster Engine Design**

The NorEaster engine uses the cam-follower technology described in Section 2.1.5 to convert the energy produced in the cylinder head into counter coaxial rotation. In a gasoline engine, a fuel-air mixture is compressed and ignited by a spark, which in turn causes the cam to rotate. In a diesel engine, a fuel-air mixture is compressed until its temperature is high enough to achieve self-ignition, at which point the cams rotate. In the current prototype, the oval shaped path, labeled "Track A" in Figure 8, rotates at half the reciprocating speed of the pistons. This relationship is a result of the two lobe design of the cam.

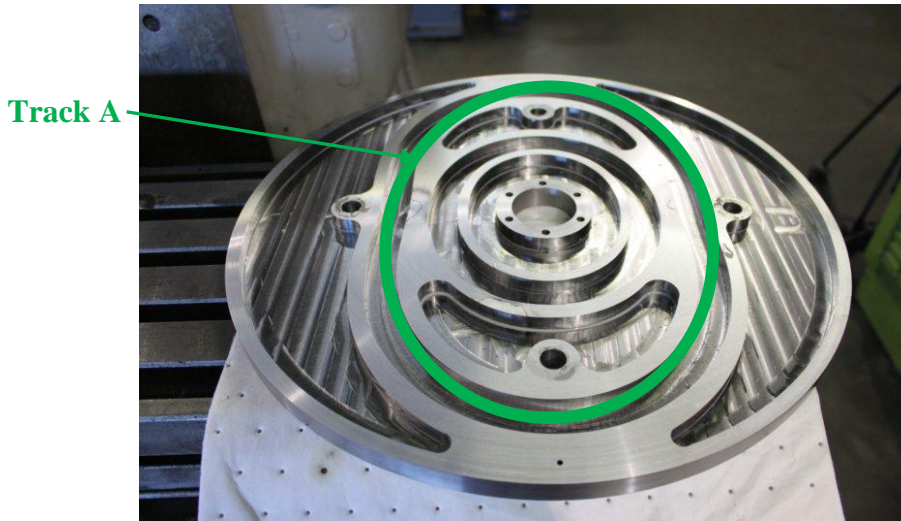


**Figure 8: The NorEaster's Existing Cam Design**

Within the engine, there are two cams that rotate in opposite directions. This counter-rotation between the cams creates the co-axial counter rotation of the rotors. The coaxial-counter rotation design is described in U.S. Patent No. 7,219,631 B1.

The NorEaster engine utilizes gearless reduction to minimize the high speed required of a typical helicopter engines. In turn, the NorEaster generates suitable rotor speeds to lift the aircraft off the ground without the assistance of external gears. The current design operates at a 2:1 gear ratio. The new engine design will operate at a 4:1 gear ratio, which helps generate high torque and at low rpm.

The NorEaster engine was designed to be perfectly balanced. The piston from the cam's motion is a pure harmonic, which means that the velocity of the pistons follows a sinusoidal curve, and the connecting rods are in pure translation, thus adding no harmonics. As the cam turns and the pistons reciprocate, the valves open and close at different points in the cycle. Additionally, the pistons and their connecting rods are not offset in the axial direction, which eliminates unbalanced moments.

The existing NorEaster was designed with various cylinder arrangements in mind. For example, the transmission case and "snowflake plate" on the existing engine, shown in Figure 9, can accommodate up to eight cylinders. Adding more cylinders to the existing design would

increase the power produced by the NorEaster and help the O’Neill Motor Company, Inc. explore various ways to optimize the engine.

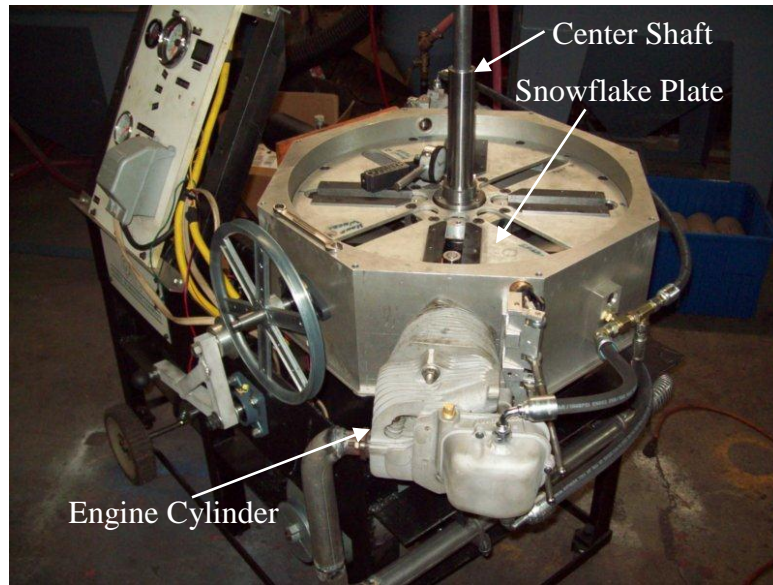


**Figure 9: View of the Snowflake Plate Inside of the NorEaster Engine**

The fully assembled prototype of the NorEaster engine can be seen in Figure 10. This was constructed by OMC before this project began.



**Figure 10: Fully Assembled NorEaster Engine**

### 2.1.7 Engine Design Optimization

In order to optimize the engine design, we determined which parameters can be adjusted. Some of these parameters include the compression ratio, bore size, cut-off ratio, and firing temperature due to different fuels. Gasoline and diesel engines are optimized in different ways. Despite these adjustable parameters, the optimized engine design must use the same helicopter blades and angle of attack to generate lift.

## 2.2 Comparison to Existing Drone Engines and Companies

The AAI RQ-7 Shadow, Reaper Drone, Predator Drone and Northrop Grumman MQ-8 Fire Scout are existing UAVs that resemble the NorEaster engine. In assessing the performance of the NorEaster engine, it is helpful to understand the existing UAV market and the competition's ability to perform.

The AAI RQ-7 Shadow is an UAV used for the U.S. Army and Marine Corps. It includes an electro-optical/infrared camera that relays video in real time via a C-band line-of-sight data link to the ground control station. While in flight, the Shadow uses a Wankel engine and can generate 38 brake horsepower (UAV Engines LTD, 2004). A Wankel rotary engine, one of the most common types of rotary engines, uses a rotor to convert pressure into rotating motion instead of using conventional reciprocating pistons.

The Reaper Drone, also known as the MQ-9, is designed for long-endurance, high-altitude surveillance. Much larger than the Shadow or Predator, the Reaper Drone has a maximum takeoff weight of 10,500 pounds (UAV Engines LTD, 2004). It utilizes a Honeywell TPE331-10 turboprop engine which outputs 950 shaft horsepower. The turboprop engine drives the propeller of the aircraft using a reducing gear. This gearing configuration allows the turbine to transform its high rpm and low torque to low rpm and high torque through gearing. Unlike large aircraft turbines, the turboprop engine's exhaust plays only a minor role in propulsion of the UAV.

The Predator Drone, or the MQ-1, is used primarily by the U.S. Air Force and Central Intelligence Agency. This UAV can take off with a maximum weight of 2,250 pounds (Military Factory, 2010). The Predator utilizes a Rotax 914F turbocharged four-cylinder engine (Military Factory, 2010). The engine is horizontally-opposed, and it can produce 115 horsepower



(Military Factory, 2010). It has a dry weight of 172 pounds, a bore of 3.1 inches, a stroke of 2.4 inches, and a displacement of 74 cubic inches (Military Factory, 2010).

The Northrop Grumman MQ-8 Fire Scout is a UAV helicopter. It is used by the U.S. Armed Forces to provide reconnaissance, situational awareness, and precision targeting for military support. The Fire Scout has a maximum takeoff weight of 3,150 pounds (Northrop Grumman, 2011). The Fire Scout is powered by a Rolls-Royce 250 turboshaft engine which produces 419.7 horsepower. The engine has a dry weight of 173 pounds (Northrop Grumman, 2011).

The Sikorsky X2, displayed in Figure 11, is a manned helicopter which was developed with a new blade configuration. The configuration has two blades, which rotate in opposite directions on the same axis, like the NorEaster engine. This allows for most of the forces to balance out and eliminates the need for a tail rotor. The X2 recently broke the helicopter speed record at nearly 300 miles per hour. It is powered by a LHTEC T800-LHT-801 turboshaft engine which produces between 1300 and 1800 shaft horsepower. It has a maximum takeoff weight of 7,937 pounds (Sikorsky, 2011). Its rotor diameter is 26.4 feet (Sikorsky, 2011).



**Figure 11: The Sikorsky X2**

The NorEaster engine incorporates the same counter rotating blade configuration seen in the Sikorsky X2 but sends power to the rotors differently. The performance of the NorEaster engine can be compared to the Fire Scout, since that engine incorporates similar design aspects (Northrop Grumman, 2011). These performance measures are provided in Chapter 4 of the report

### 3.0 Methodology

The combination of several research methods allowed us to determine how to model the NorEaster engine in a computer simulation, and in turn helped the O'Neill Motor Company Inc. determine the engine's output power. The approximate weight of the existing engine prototype was determined and used to calculate the power to weight ratio. Additionally, several tests were run to analyze the current engine's performance. Research on the NorEaster engine can be used to understand the current limitations of the engine and determine how to best maximize its output power.

### 3.1 Free Body Diagram of the NorEaster Engine

The free body diagram, shown in Figure 12, demonstrates where the forces are exerted on the cams in the NorEaster engine. In this example, the cam turns clockwise. The forces acting on the cam are labeled in the legend on the figure.

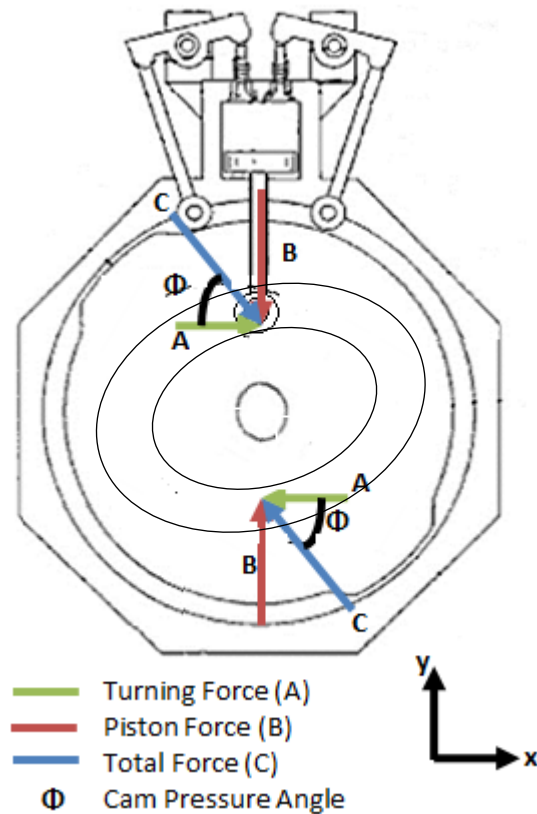


Figure 12: Free Body Diagram of the NorEaster Engine

The angle,  $\phi$ , represents the pressure angle of the cam. This rotation is due to the sum of all of the forces in their respective directions. The piston force is exerted through the center of the cam. Future designs can maximize the total force by increasing the piston force and the turning force. Each of these forces is dependent upon a combination of engine parameters such as the bore size, compression ratio and temperatures within the cylinder.

### 3.2 Weight Calculations

<b>Current Two Cylinder Engine</b>			
	Individual Weight (lbs.)	Number of Pieces	Total Weight (lbs.)
<b>Octagon Cover</b>	13	2	26
<b>Cam</b>	31	2	62
<b>Snowflake Plate</b>	6	2	12
<b>Engine Cylinder</b>	9	2	18
<b>Aluminum Shell</b>	55.88	1	55.88
<b>Nuts and Bolts</b>	--	--	
<b>Gearbox Case</b>	--	1	
<b>Gears</b>	--	--	
<b>Piston</b>	--	2	
		<b>Total Engine Weight</b>	<b>173.88</b>

Table 2: Current Two Cylinder Engine Component Weights

Several components of the existing engine were weighed within an accuracy of one pound. SolidWorks was used to estimate the weight the aluminum shell. These can be seen in Table 2. The top octagon cover, one cam, one engine cylinder and one snowflake plate were removed from the engine and measured on a scale. The total weight of the current engine, excluding the gearbox case, gears, pistons, nuts and bolts, is 173.85 pounds.

Because all of the calculations performed in Chapter 4 are based on new engine designs, these weight calculations need to be adjusted. The NorEaster Design Group provided weight calculations for a gasoline and diesel engine with differing bores. This information can be found in Table 3.

<b>Bore Size</b>	<b>Gasoline Engine (lb)</b>	<b>Diesel Engine (lb)</b>
<b>3 inches</b>	812	812
<b>4 inches</b>	842.5	842.5
<b>5 inches</b>	875.7	875.7

Table 3: Weights from the NorEaster Design Group's SolidWorks Models.

### 3.3 Cylinder Compression Ratio Measurement

The compression ratio of the existing engine cylinders was determined by dividing the volume of the cylinder at bottom-dead center by the volume at top-dead center. The volume of the cylinder was measured in two parts: volume where the stroke of the piston occurs and volume where the stroke of the piston does not occur. The stroke and bore for the existing engine are both three inches. The stroke-volume for the existing NorEaster engine is 21.21 cubic inches.

The volume of the cylinder between top dead center and the cylinder walls was measured by determining the volume of liquid that fit in the top of the cylinder. This is the volume of space that the compressed air fills when it is ignited. The top of the cylinder was secured in a vise with the open head facing the ceiling. A level was used to make sure that the cylinder was always measured in the same position relative to the ground and that all measurements were accurate. Water was poured from a graduated cylinder into the top of the cylinder head until a meniscus formed and the amount of water that had been poured into the cylinder head was measured. Five trials were completed in order to obtain an average volume of 59.8 mL (Table 4).

<b>Test</b>	<b>Measured Volume (mL)</b>	<b>Additional Calc. Vol. (mL)</b>	<b>Final Vol. (mL)</b>
<b>1</b>	53.5	5.4	58.9
<b>2</b>	58.5 (error)	5.4	63.9
<b>3</b>	54	5.4	59.4
<b>4</b>	51	5.4	56.4
<b>5</b>	55	5.4	60.4
		<b>Average</b>	<b>59.8</b>

Table 4: Measurements to Calculate the Volume when the Piston is at Top Dead Center

Therefore, the volume of the piston at top-dead center is 59.8 mL. The volume of the piston at bottom-dead center is 407 mL. The compression ratio is 7:1.

### 3.4 Mechanical Compression Test

A mechanical compression test was run on both cylinders to ensure that the compression in the cylinders was sufficient enough to run a pressure test. A compression tester kit was connected to each of the cylinders at the spark plug holes and turned over the engine using the electric starter motor. Three trials were run for each cylinder to obtain an average pressure. The average mechanical cylinder compression for one cylinder head was 113 psi, and 115 psi for the other cylinder head.

### 3.5 Blade to Engine Relationships

In order to ensure that the NorEaster functions at optimized conditions, we analyzed the design of the propeller blades. We assessed the limitations on the diameter of the rotor blades and analyzed how they vary with revolutions per minute.

#### 3.5.1 Maximum Blade Diameter Compared to Engine RPM

The maximum possible revolutions per minute of the NorEaster engine were calculated. This calculation depends on the speed of the blades at their tips. The wing tip speed of the helicopter blade must remain subsonic in order to eliminate the possibility of vibrations that could disturb flight.

Using the information on the maximum rpm of a helicopter engine, the maximum helicopter blade radius was calculated. The limitation on the speed of the tip of the helicopter blade was calculated by dividing the speed of sound by a safety factor of 1.2 and subtracting the maximum forward speed. The speed of sound is 761.2 mph at sea level and the fastest helicopter has a top speed of nearly 300 mph. As the helicopter increases its altitude, the maximum achievable speed will decrease. This calculation can be seen in Appendix A.

Figure 13 shows the engine rpm versus the rotor length. The curve, marked with squares, is the upper extreme representation of data because it does not take into account a safety factor or the speed of the helicopter. The other three curves take into account a safety factor of 1.2 and a maximum forward speed of 100 mph, 200 mph and 300 mph. If the rotor diameter is assumed to be 12 feet (1.83 m radius), the maximum engine speed is 780 rpm, 1013 rpm and 1246 rpm for a maximum forward speed of 300 mph, 200 mph and 100 mph respectively. The engine's pistons would feel like the engine was rotating four times as fast due to the internal 4 to 1 ratio.

Therefore, the performance of the pistons would be compared to maximum engine rpm values of 3120, 4052, and 4984 for the three forward speeds of 300 mph, 200 mph and 100 mph respectively.

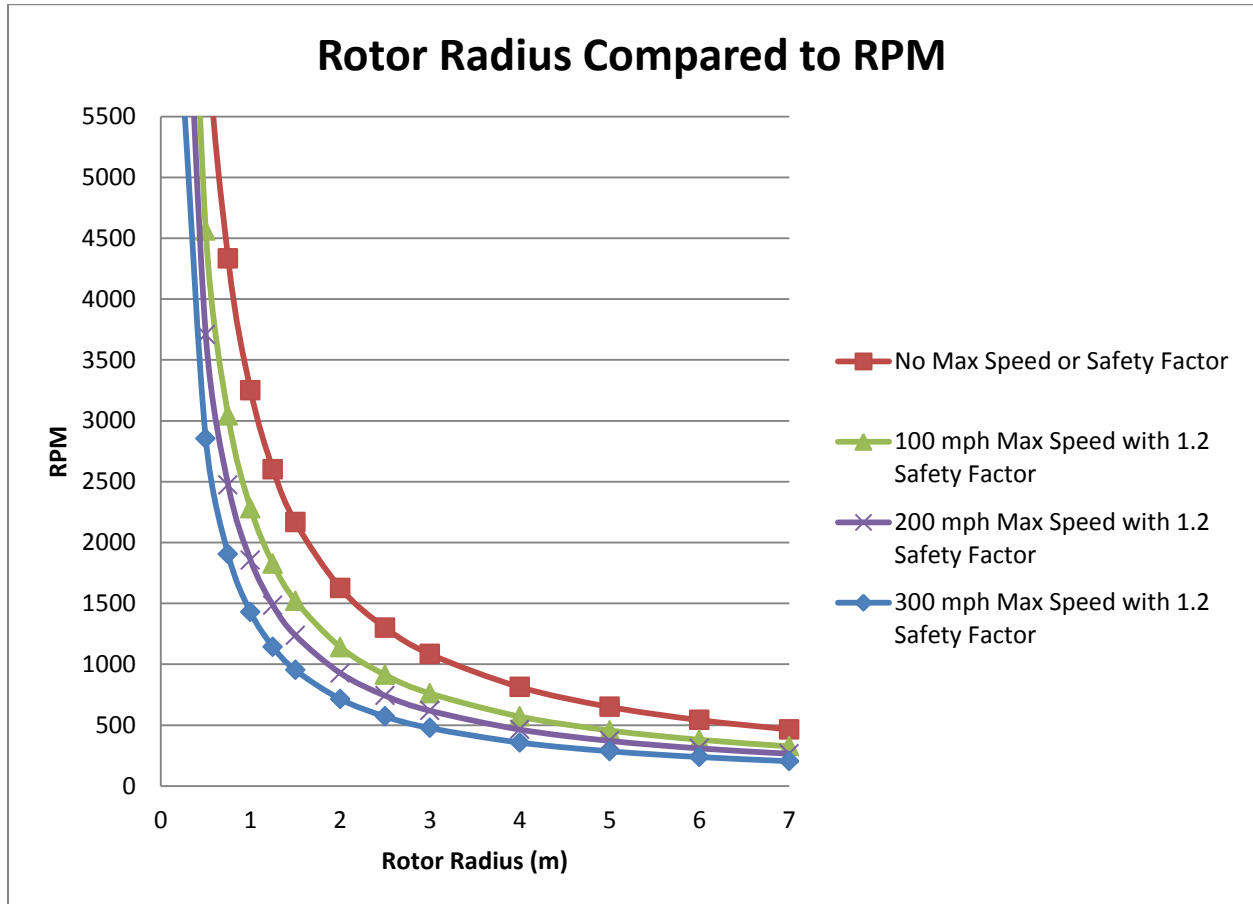
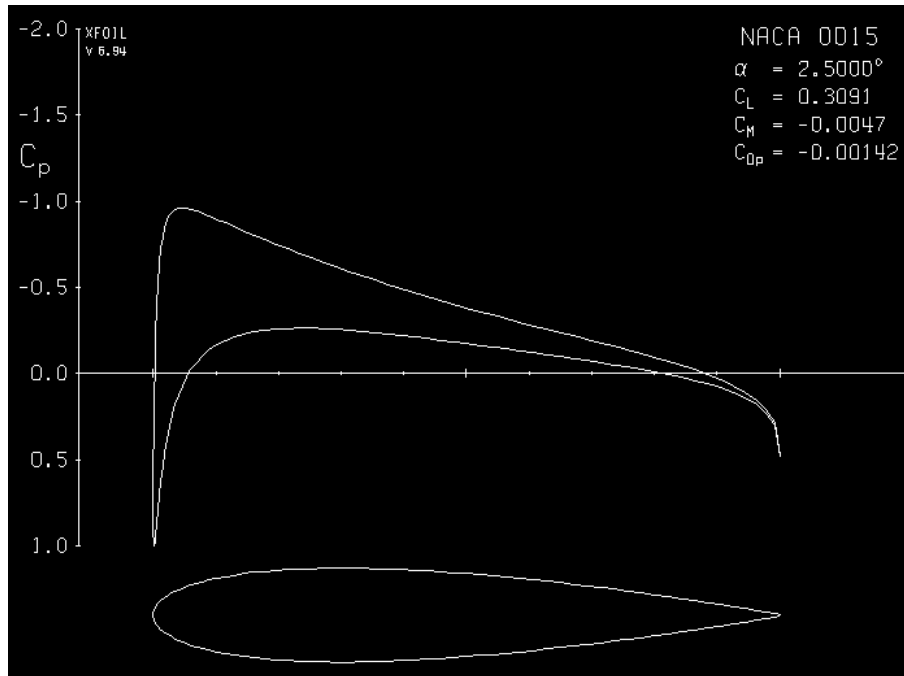


Figure 13: Graph of the Propeller Blade Diameter vs. the Potential Revolutions per Minute

### 3.5.2 Limitations of NACA0015

Figure 14 shows a screenshot from MIT’s XFOIL program. This program calculates the lift and drag coefficients at a given angle of attack. The graph shown in Figure 14 shows the curve of a 2.5 degree angle of attack. In this example, the drag coefficient is -0.00142, and the lift coefficient is 0.3091.



**Figure 14: Image of the NACA 0015 Providing Lift and Drag Coefficients (MIT XFOIL)**

Figure 15 shows the lift and drag coefficients for a NACA 0015 airfoil. As demonstrated in this figure, the lift to drag ratio ranges from 0 to 100. Both the lift and drag coefficients are a function of the angle of attack. The drag coefficient increases exponentially, until it reaches its stall point at an angle of attack of 20 degrees. The lift coefficient increases linearly until it reaches a stall point at an angle of attack of 20 degrees. Therefore, a NACA 0015 airfoil will cause an engine to stall at approximately 20 degrees.

Wind tunnel measured data coefficient of lift and drag

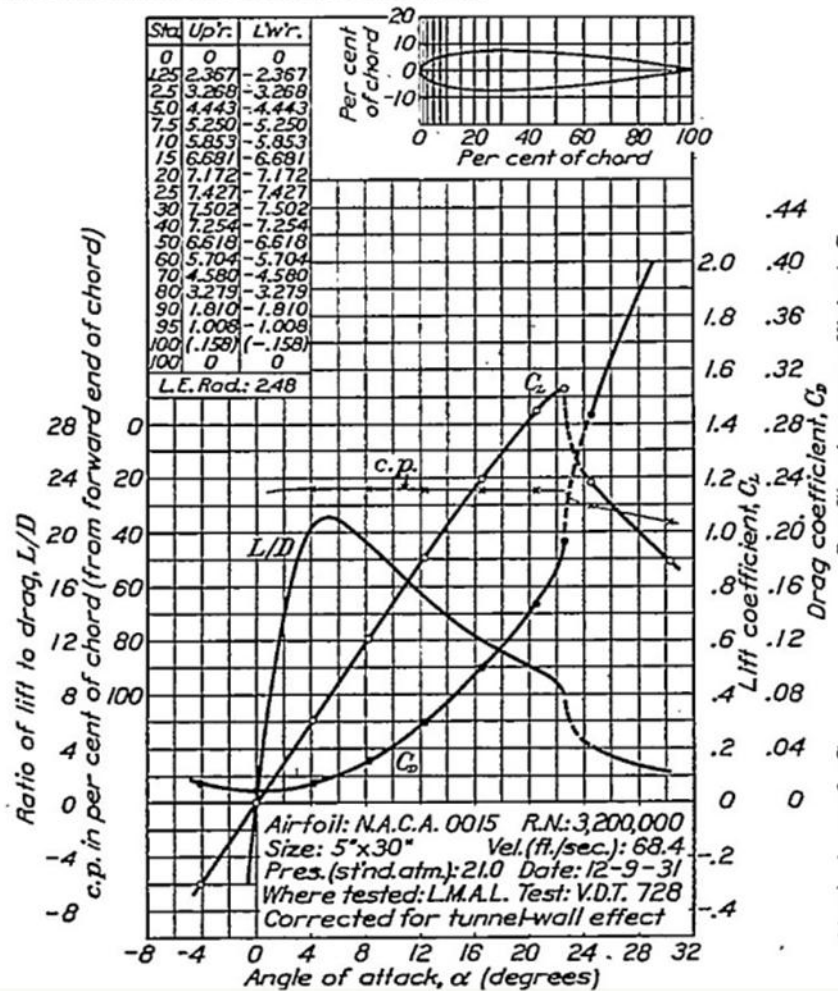


Figure 15: Lift and Drag Coefficients of NACA 0015 at Varying Angles of Attack (CSEE)

In order to compare the NorEaster engine with similar helicopter engines, the lift force is an important parameter to assess. Calculating the lift force for a helicopter blade is a complicated procedure that requires assuming values for many of the engine's design characteristics. This rotor design method is often referred to as the blade element method. In order to avoid these complexities, the lift force on a helicopter can be determined by utilizing the actuator disk model. Under the actuator disk model, the blade of a helicopter is analyzed as the rotor blades are spun, so the model resembles that of a flat disk (Scott, 2001). Increasing the weight of a helicopter and its engine will increase the disk loading.

The lift force on a helicopter is dependent upon two factors. First, as the air comes into contact with the helicopter blades that form the actuator disk, it is deflected downward. Second,



Bernoulli's principle states that air flowing over a curved surface gathers speed but loses pressure. As a result, low pressure exists above the actuator disk. The high pressure that builds up below the disk wants to move towards the low pressure, and in the process of this movement, lift is generated (Scott, 2001).

For an airfoil, the lift force can be calculated by:

$$L = \frac{1}{2} \rho v^2 A C_L$$

In this equation, the density of air,  $\rho$ , is multiplied by the square of the true air speed,  $v$ , the plan form area,  $A$ , and the lift coefficient,  $C_L$ , at the desired angle of attack. In order to calculate this force, the desired angle of attack of the desired air speed must be decided. These values typically depend on existing designs in the engine market. The parameters can be optimized to a certain extent, but they cannot exceed the angle of attack at which the engine would stall out. For the NACA 0015 airfoil, the maximum angle of attack is 20 degrees. As a result, the lift force must occur at an angle of attack of less than 20 degrees and at a true air speed that is competitive with existing technologies.

### **3.6 Dynamometer Testing**

This section of the report discusses the dynamometer testing that was performed on the current NorEaster Engine.

#### **3.6.1 Procedure**

A purpose-built dynamometer was created with the assistance of the O'Neill Motor Company, Inc. to gather experimental data on the NorEaster's current output power. A DC motor was used as a generator. We recorded voltage across four resistors, shown in Figure 16, and measured the current through the circuit.



**Figure 16: Circuit Board Used for the Dynamometer Test Performed on the NorEaster Engine**

The current was measured with an ammeter. The voltage was measured with a voltmeter. The rpm of the engine was measured with a tachometer. In an effort to obtain accurate and consistent data, the current, voltage and engine rpm were recorded when there was a no-slip condition on the belt connected to the generator.

Once all of the data was recorded, the power was calculated using the equation,

$$P = IV$$

Where  $P$  represents power measured in Watts;  $I$  represents current measured in amperes; and  $V$  represents voltage measured in volts. The power was converted from Watts to horsepower and a linear regression was calculated to compare the output power to the engine rpm. For all computations, see Appendix B.

### **3.6.2 Dynamometer Test 1 Results**

Once all data were collected and calculated, the rpm data were compared to the corresponding horsepower data, listed in Table 5.

RPM	Horsepower
1050	0.68
600	5
500	1.87
760	1.67

Table 5: Comparison of RPM with Corresponding Horsepower

As displayed in Figure 17, there is a negative correlation between horsepower and RPM with a slope of -0.004561 and a y-intercept of 5.623. This means that the engine's output power decreased 0.4561 horsepower for every increase in 100 rpm. It was concluded that the results of this test were not representative of the engine's capabilities because the engine was not running well during this test. A negative slope represents that the input to output power is in an inverse ratio which should not be the case. Also, the line of best fit for the data points has a low  $R^2$  value of 0.343. For a trend-line to be representative of the data in a scatter plot, the  $R^2$  value needs to be between 0.970 and 1.000.

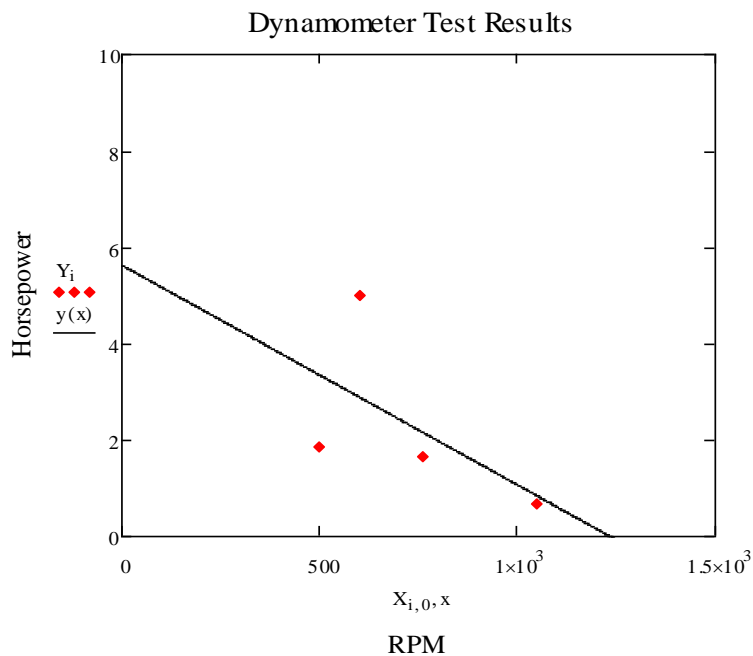


Figure 17: Graph Comparing Horsepower to RPM

The variation in the collected data may be due to several factors. From examining the engine during the test, it was determined that only one of the two cylinders in the NorEaster fired. This is a mechanical failure that must be fixed in order to collect accurate data. Secondly, the ammeter was did not accurately read any values below 10 amps, which resulted in invalid

data. Additionally, it was very difficult to confirm a no-slip condition when the friction of the belt on the motor/generator was only being judged by sight and touch. These variables, along with the typical human error in reading devices such as ammeters, tachometers, and volt meters, add up. Finally, in the post-procedure inspections, it was determined that there was too much fuel in the engine during the combustion stage, since each of the brand new spark plugs was covered in soot after only having been used for approximately twenty minutes. The combination of these errors account for the low values recorded.

### 3.6.3 Dynamometer Test 2 Results

Due to all of these inaccuracies, a second test was performed to measure the engine's actual power, under different circumstances. When executing the second dynamometer test, several improvements were made to the procedure resulting in more accurate data. First, both cylinders were functioning properly with the correct fuel to air ratio. Additionally, a more accurate ammeter was used to ensure that all readings below 10 amps were as close to the actual current as possible. Once all data was collected and calculated, the rpm data was compared to the corresponding horsepower data, listed in Table 6.

<b>RPM</b>	<b>Horsepower</b>
800	0.95
900	0.94
1000	1.07
1000	1.09
1100	0.98
1100	1.01
1200	1.09
1200	1.17

**Table 6: Comparison of RPM with Corresponding Horsepower**

As shown in Figure 18, there is a positive correlation between horsepower and rpm with a slope of 0.389 and a y-intercept of 0.623.

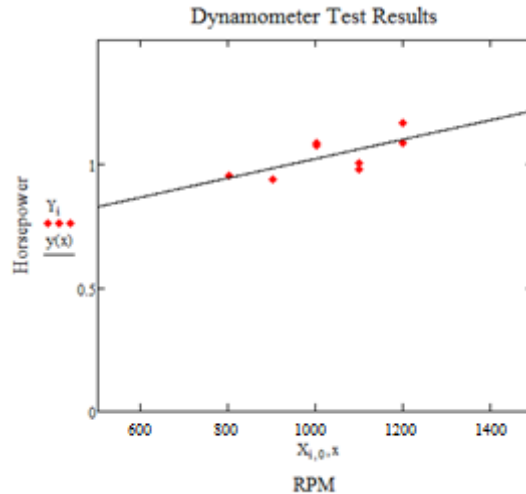


Figure 18: Graph Comparing Horsepower to RPM

This means that the engine's output power increased by 0.389 horsepower for every increase in of 100 rpm. The line of best fit for the data points has a low  $R^2$  value of 0.476, which is not within the desired range. Unfortunately, the engine was still not running at its optimal performance, and the results still have some error in them.

### 3.7 Pressure Transducer Test

This section of the report provides detail on how the pressure inside one of the cylinder heads of the NorEaster engine was measured.

#### 3.7.1 Procedure

In order to measure the pressure in the cylinder head as the engine fired, a piezoelectric Dytran pressure transducer Model 2200C5 was installed flush to the inside surface of the cylinder head. The pressure transducer's signal, measured in pC/psi, was relayed to a PCB Charge Amplifier Model 462S05 as shown in Figure 19, to convert the signal to mV/psi. The signal from the charge amplifier on the HP Dynamic Signal Analyzer in mV was recorded as a function of time, shown in Figure 20. The mV reading was converted to psi using a 6.22 mV/psi conversion factor, which was determined by the calibration method described in the following paragraph.



Figure 19: PCB Charge Amplifier Model 462S05

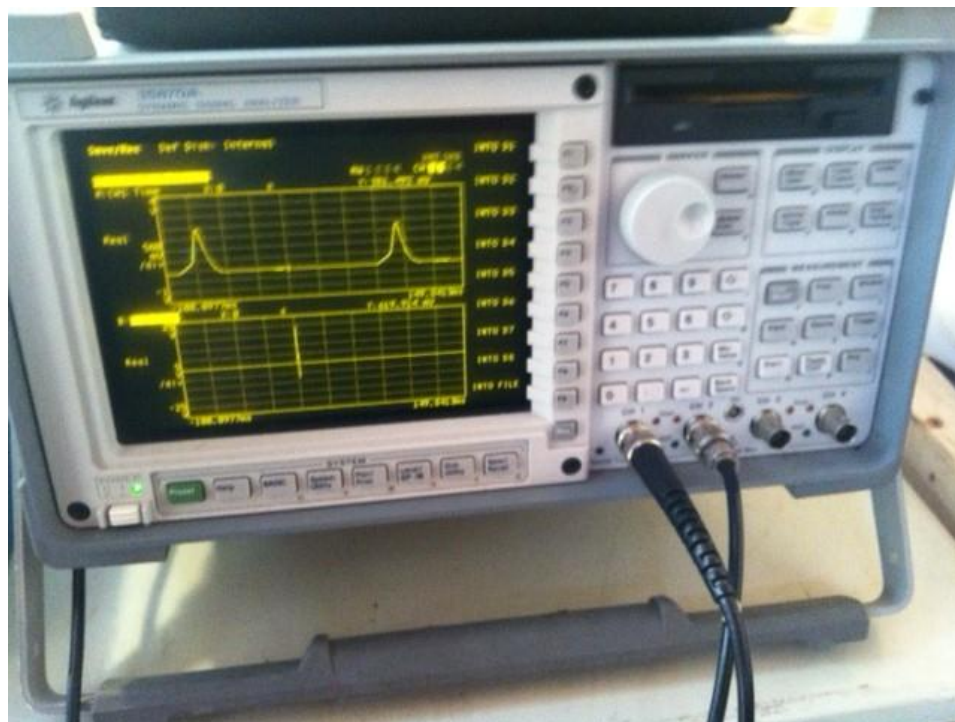


Figure 20: HP Signal Analyzer

In order to calibrate the Dytran pressure transducer, a strain gauge pressure transducer, model BLH-PR034, and the Dytran transducer, shown in Figure 21, were simultaneously subjected to the same static pressure from an air hose. The pressure was released suddenly and data from both pressure transducers, Dytran (V) and Strain Gauge (psi), were recorded as a function of time. The calibration factor of the Dytran pressure transducer was calculated by dividing the change in voltage of the Dytran pressure transducer by the change in psi of the strain gauge pressure transducer. Three calibration tests were run to minimize error yielding an average calibration factor of 6.22 mV/psi.



**Figure 21: The Valve and Gage Used to Calibrate the Pressure Transducer**

In order to pinpoint the piston's location at TDC in relation to the pressure readings, a Shaft Encoder Model 776, shown in Figure 22, was mounted on the outer rotating shaft that is attached to the cam. The signal from the shaft encoder was recorded simultaneously with the pressure transducer in the same signal analyzer as a function of time.

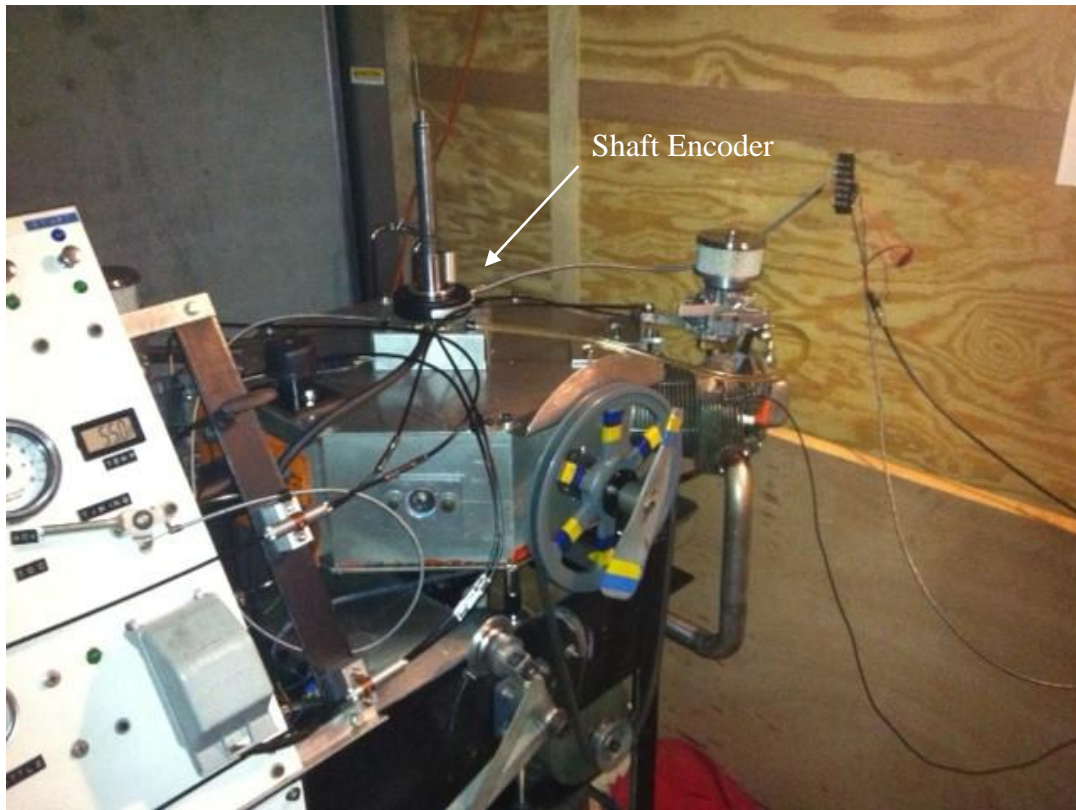


**Figure 22: Shaft Encoder Model 776 Mounted on the NorEaster Engine**

The first test was completed without the cylinder heads firing, allowing for a comparison between the pressure test and compression test data. Two more relevant tests were performed and recorded. The data was collected taking pressure measurements at a rate of 16,384 Hz. After the first test, we noticed that only the cylinder with the pressure transducer in it was firing. The first test results were compared to the results of a second test in which the spark plug was removed from the cylinder that was not firing.

### **3.7.2 Pressure Transducer Test Results**

Figure 23 shows the pressure measurements of the motoring NorEaster engine. The pressure data is displayed by the line labeled A, and the shaft encoder index is represented by the line labeled B. The sharp increase in the index represents when the piston is at top-dead center during the power stroke. The peak values of each pressure curve demonstrate that the maximum pressure during compression is approximately 139.9 psi. A pressure test was run with the engine firing, shown in Figure 24, using the same setup as the compression test. As exhibited in the graph, the engine fired after top-dead center at a pressure of 75 psi. We noticed a significant



discrepancy between the peak compression values in these two tests. These tests were performed one after the other with the same setup. At this time the team does not have a solution for why there is a significant difference in compression pressures between the two tests. Also, both of the compression pressures measured with the Dytran pressure transducer were different than the 113.5 psi value measured with the mechanical compression tester. Since the two methods of testing the compression pressure in the cylinder were different, it is reasonable for there to be a variance in the compression pressures. However, more testing would need to be done to determine why the difference between the measured pressures was so large.

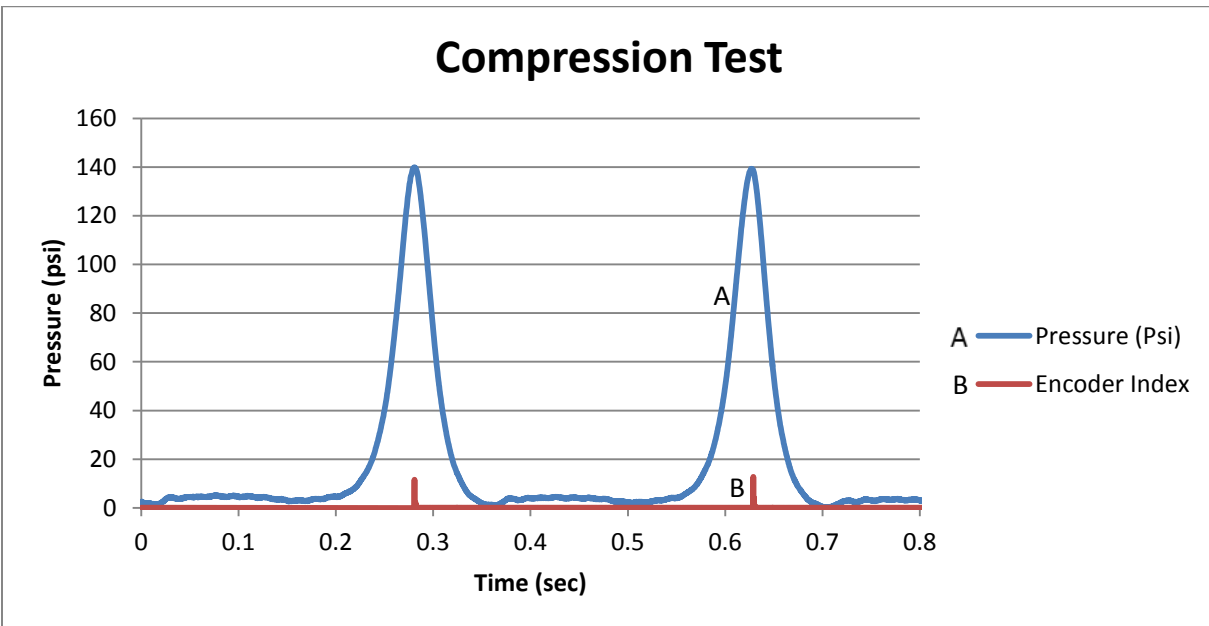


Figure 23: Pressure Data: Compression Test

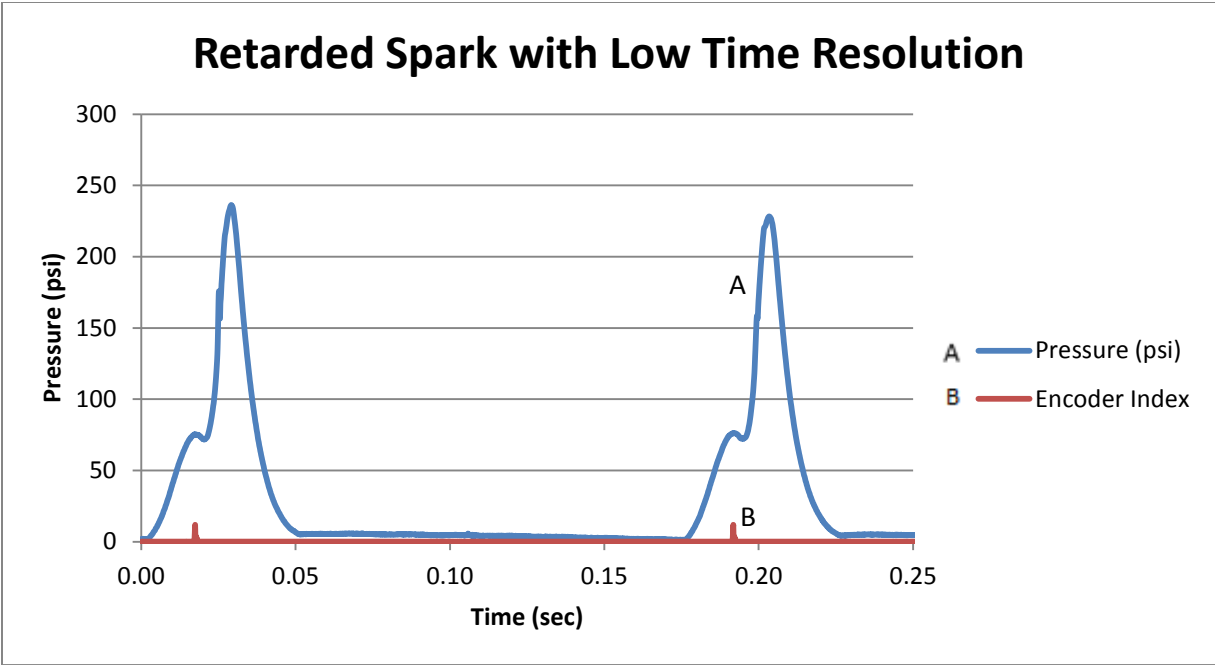


Figure 24: Pressure Data: Retarded Spark with Low Time Resolution

Figure 25 shows the recorded pressures during the two trials for a cylinder firing when the piston was at TDC. The first trial, labeled B, included both spark plugs, and the second trial, labeled A, included only one spark plug in. Again the shaft encoder, labeled C, was used to determine where top-dead center occurred during the tests. The time scale resolution was set to 16,384 Hz during these two trials, and the greatest time scale in which the pressures from two compression strokes were recorded. This allowed for more accurate pressure measurements. The data collected from one test to the next is consistent and the difference in the peak pressure with one spark plug or two is negligible. The average maximum pressure was 341.1 psi.

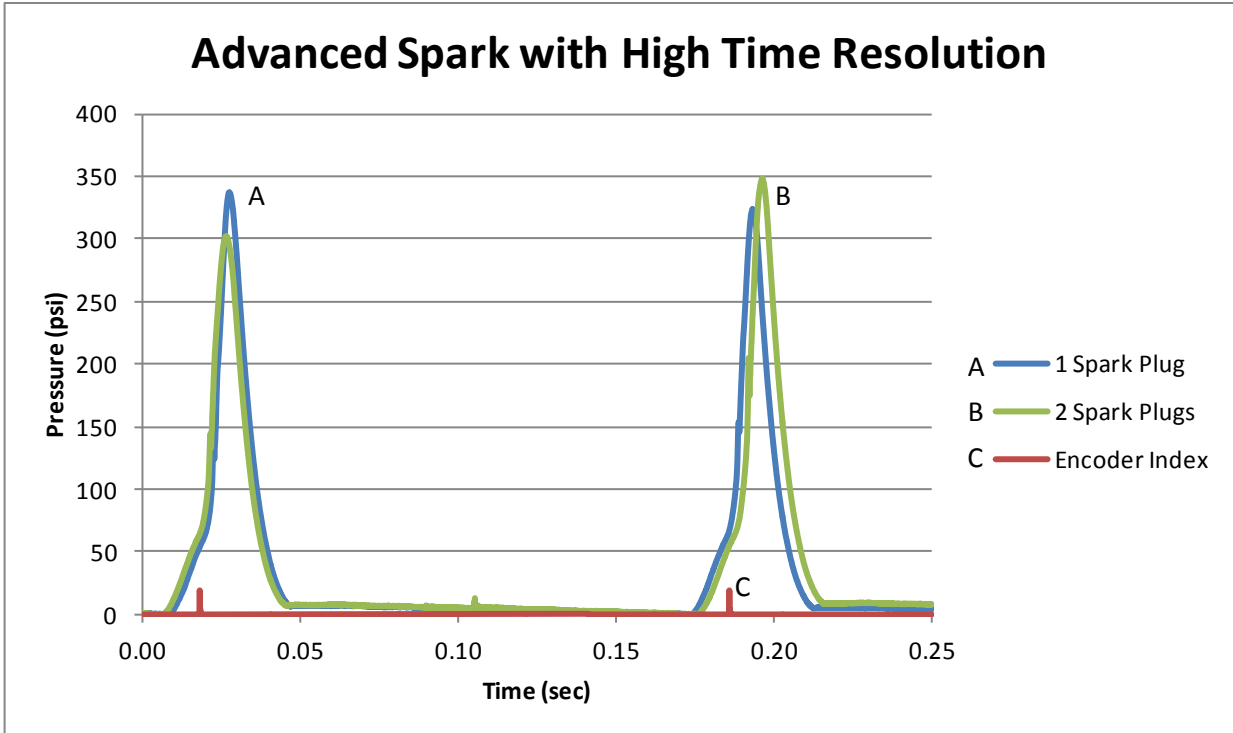


Figure 25: Pressure Data: Advanced Spark with High Time Resolution

The turning force, displayed in Figure 26, was calculated from the product of the pressure from the pressure test, the area of the piston, and the tangent of the pressure angle. From this calculation, the maximum force which was turning the cam was 2173 N. To find the torque, the turning force was multiplied by the radius of the cam at that given time. The maximum torque from the torque graph, shown in Figure 27, for the calibration was 333.2 N\*m.

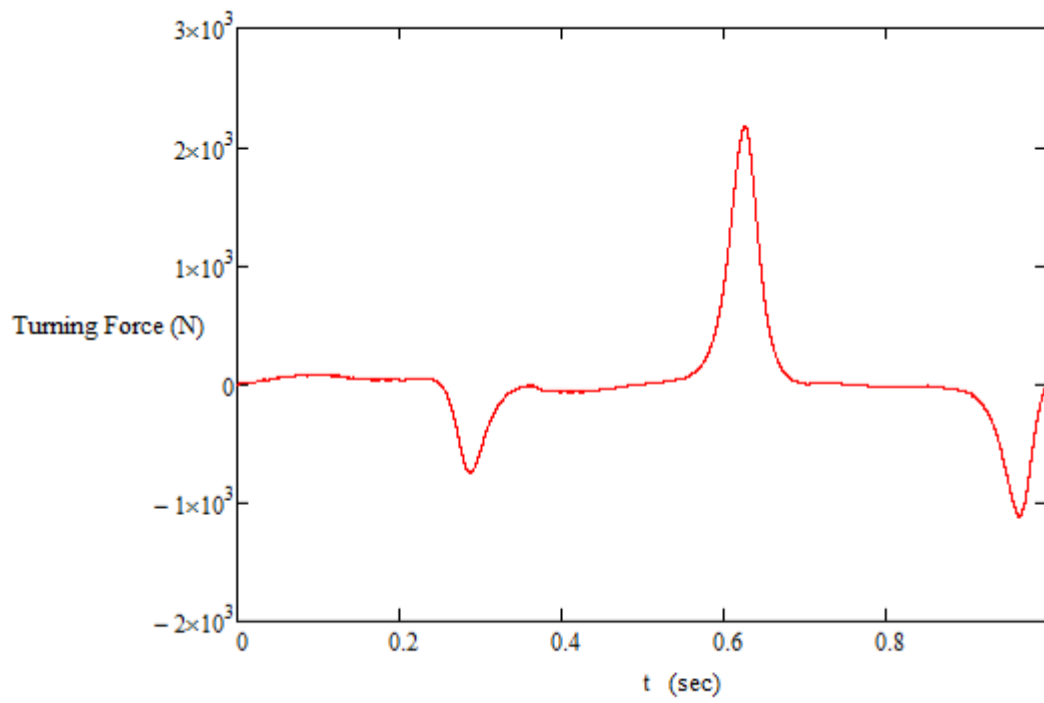


Figure 26: Calibration Turning Force

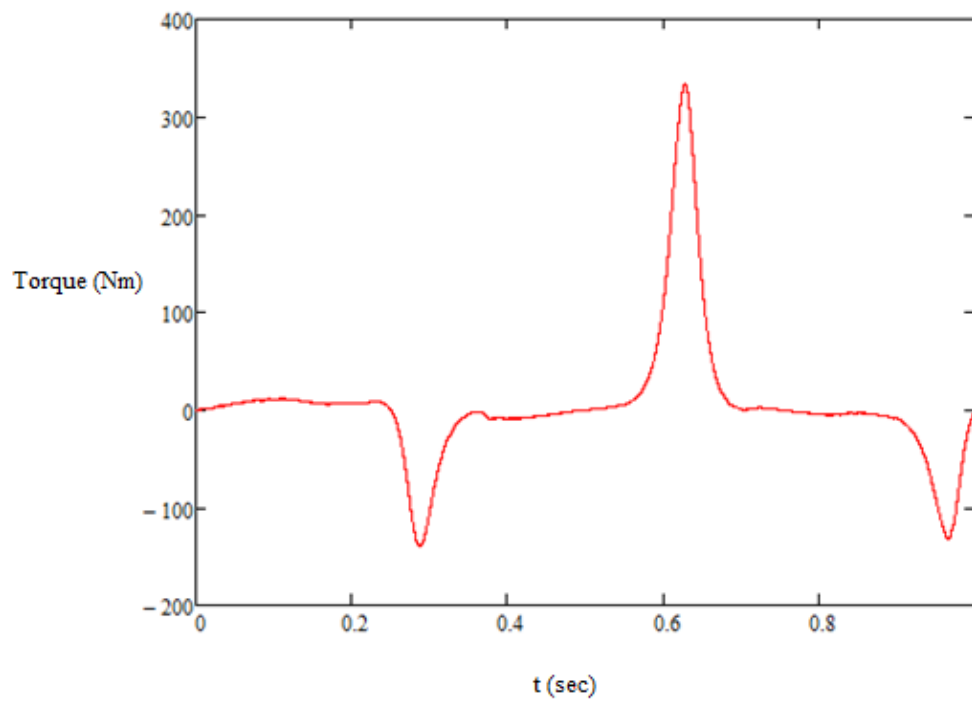


Figure 27: Calibration Torque

For the remaining trials, we manually calculated the maximum turning force and torque. A summary of these values for the other trials are shown in Table 7.

	<b>Max Pressure (psi)</b>	<b>Turning Force (N)</b>	<b>Torque (N*m)</b>
<b>Calibration</b>	139.1	2173	333.2
<b>Retarded Spark</b>	265.8	4151	636.6
<b>Somewhat Advanced</b>	263.1	4109	630.1
<b>Advanced</b>	347.6	5428	832.5
<b>Advanced 1 Plug</b>	338.1	5280	809.7

Table 7: Pressure, Turning Force, and Torque Summation

## 4.0 Results

The following section of the report provides conclusions and recommendations for a future NorEaster engine design. In order to assess the possibilities for the NorEaster engine, we developed two mathematical models to analyze the differences between a gasoline and diesel engine. The military has expressed a minimum desired power to weight ratio of 0.5. Upon analyzing these variables, we developed several conclusions about future designs for the NorEaster engine.

### 4.1 Gasoline Engine Results

The mathematical model we used to analyze the power to weight ratio of a gasoline engine design varies as a function of the firing temperature, the compression ratio and the bore size. For gasoline engines, the firing temperature typically ranges from 1600 K to 2000 K (Moran and Shapiro, 2011). At temperatures beyond this point, the cylinder will get too hot and would potentially melt. Figure 28 demonstrates how the power to weight ratio varies with the firing temperature. The line labeled A shows the power to weight of the engine at a compression ratio of 10 and a bore of 4 inches. The line labeled B shows the power to weight ratio at a compression ratio of 6.8 and a bore of 4 inches. In both circumstances, the power to weight ratio increases as the firing temperature increases.

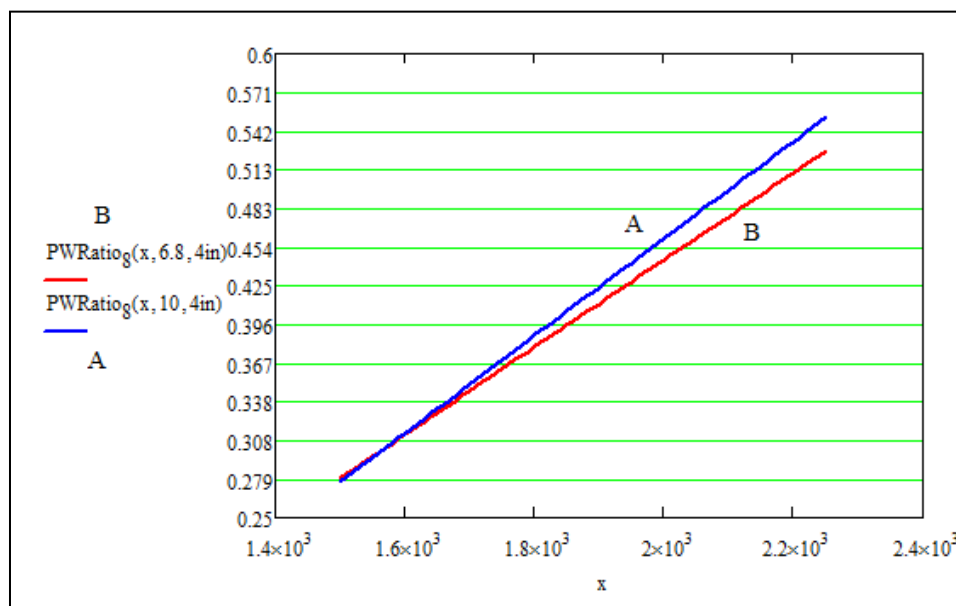


Figure 28: Power to Weight Ratio as a Function of Firing Temperature

The compression ratio of a gasoline engine typically ranges from 6.6 to 12 (Gotoh and Motoyama). Figure 29 demonstrates how the power to weight ratio varies with the compression ratio. The line labeled A occurs at a firing temperature of 1600 K and a bore of 4 inches. The power to weight ratio reaches a maximum of 0.315 at a compression ratio of approximately 9. The line labeled B occurs at a firing temperature of 2000 K and a bore of 4 inches, but here a maximum power to weight ratio of 0.463 is achieved at a compression ratio of approximately 12.5. This figure demonstrates that increasing the compression ratio will increase the power to weight ratio, until the relative maximum for a specified firing temperature is achieved.

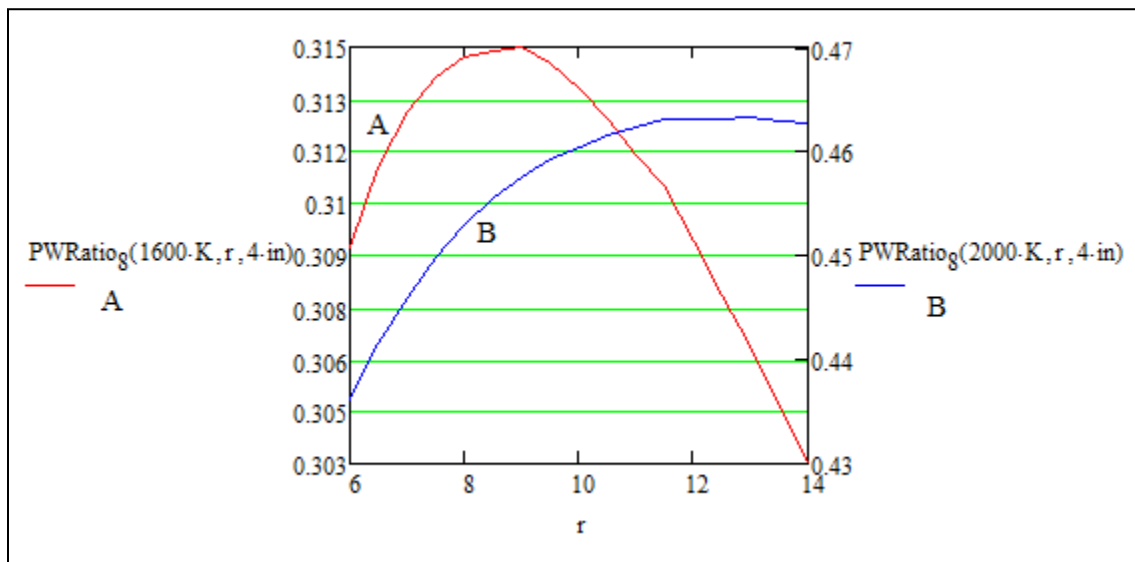
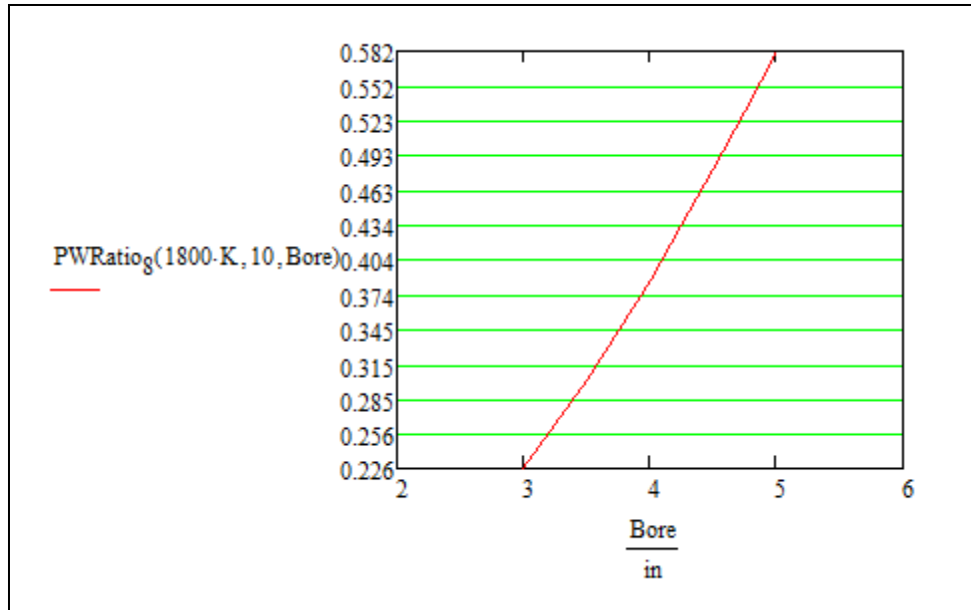


Figure 29: Power to Weight Ratio as a Function of Compression Ratio

The NorEaster engine's current bore size ranges from 3 to 5 inches. Figure 30 demonstrates how the power to weight ratio varies with bore size. This relationship is graphed at a firing temperature of 1800 K and a compression ratio of 10. The graph shows that by increasing the bore size in the range of 3 in to 5 in, a higher power to weight ratio can be achieved.



**Figure 30: Power to Weight Ratio as a Function of Bore Size**

Additionally, the weight of the engine is dependent upon the bore. The NorEaster Design team gave us the weight from their calculations of a 4 inch bore NorEaster engine experiencing diesel forces. Figure 31 demonstrates the calculation that was used to estimate the weight of a 3 inch and 5 inch engine. The total weight of the engine is calculated under the assumption that everything aside from the cylinder will not change drastically by increasing the bore size. Wall thickness is assumed to be 0.25 inches and the thickness of the top of the cylinder,  $t_c$ , is assumed to be 0.75 inches. The length of the cylinder was measured to be 12 inches. Figure 32 is a two-dimensional cross-section of the cylinder. As a result of this equation, the power to weight ratio is more accurate for different bore sizes.



$$p := 7.8 \frac{\text{gm}}{\text{cm}^3} = 7.8 \times 10^3 \frac{\text{kg}}{\text{m}^3} \quad t := 0.25\text{in} \quad t_e := 0.75\text{in} \quad L := 12\text{in}$$

$$\text{Addition}_{\text{per.cylinder}}(\text{Bore}) := p \cdot \frac{\pi}{4} \left[ \left[ (\text{Bore} + 2t)^2 - \text{Bore}^2 \right] \cdot (L - t_e) + \left[ (\text{Bore} + 2t)^2 \cdot t_e \right] \right]$$

Known Weight at Known Bore

Known<sub>weight</sub> := 812lbm      **Weight = Known Total Engine Weight**

Known<sub>Bore</sub> := 3in

$$\text{Weight}_g(\text{Bore}) := \text{Known}_{\text{weight}} - 8 \cdot \text{Addition}_{\text{per.cylinder}}(\text{Known}_{\text{Bore}}) + 8 \cdot \text{Addition}_{\text{per.cylinder}}(\text{Bore})$$

Figure 31: Equation to Calculate Weight as a Function of Bore Size

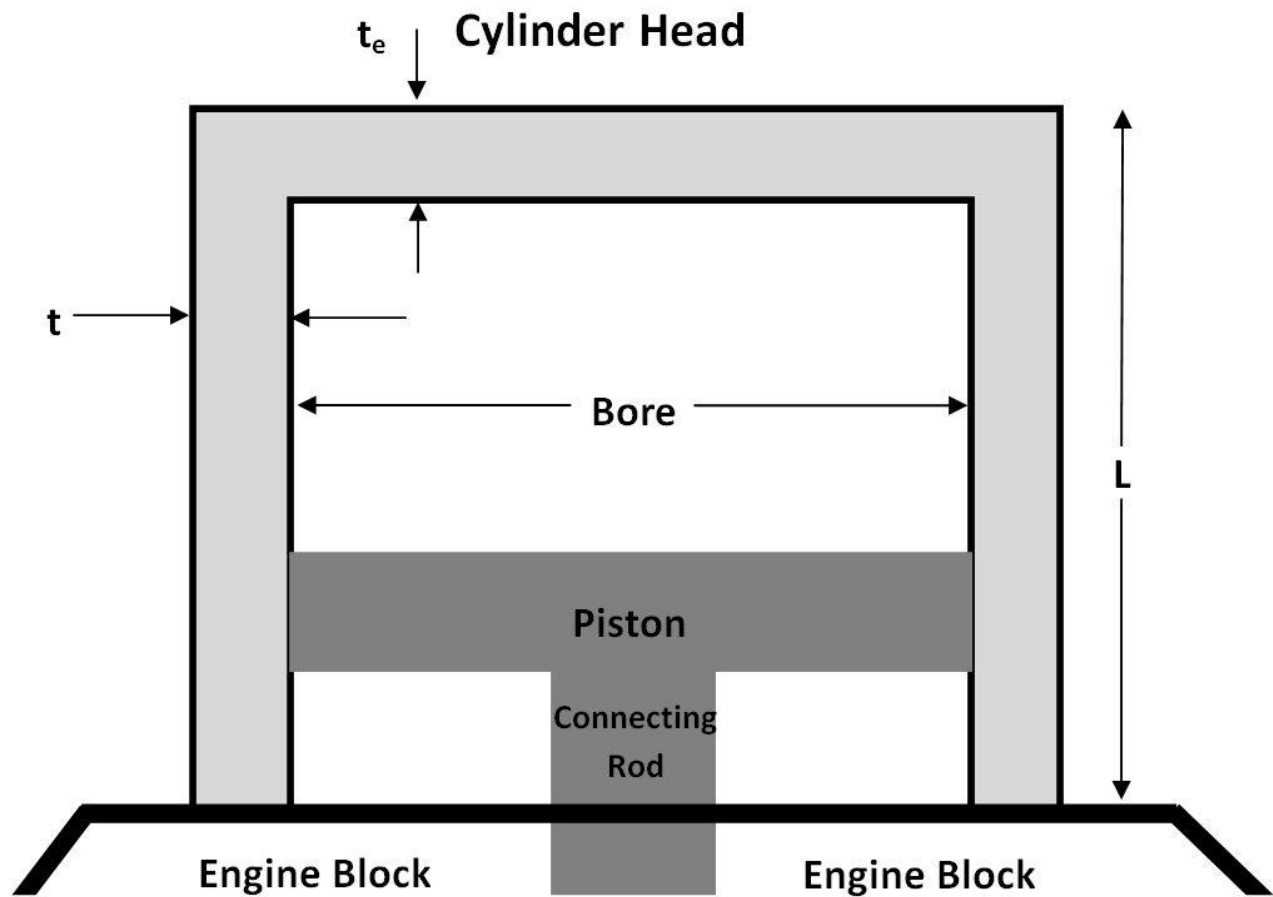


Figure 32: A 2 dimensional cross-section of a cylinder

### 4.1.1 Current Gasoline Engine Results

Our model predicts a power to weight ratio of 0.259 for an eight cylinder Army head gasoline NorEaster engine. This would occur at a measured bore of 3 inches, a compression ratio of 6.8 and a firing temperature of 2000 K. This calculation can be seen in Appendix C.

We expect a new NorEaster engine design to be able to achieve a power to weight ratio of approximately 0.46 with a 4 inch bore, a 3 inch stroke, a compression ratio of 10 and a firing temperature of 2000 K.

### 4.2 Diesel Engine Results

Diesel engines have a higher efficiency than gasoline engines, and diesel fuel is non-explosive. The ideal efficiency for a diesel engine is 56% (Office of Energy Efficiency and Renewable Energy, 2003). However, an average achievable efficiency for a diesel engine is 45% (Office of Energy Efficiency and Renewable Energy, 2003). Therefore, we performed a mathematical analysis for a diesel NorEaster engine.

The mathematical model that was used to analyze the power to weight ratio of a diesel engine design varies as a function of the cut-off ratio, the compression ratio and the bore size. The cut-off ratio represents the ratio of the volume in the cylinder at the start of ignition to the volume at the end of ignition (Engineering Software). For diesel engines, the cut-off ratio typically ranges from 1.5 to 3.5 (Engineering Software). Figure 33 demonstrates how the power to weight ratio varies with the cut-off ratio  $r_c$ . The solid line depicts a compression ratio of 20 and a bore of 4 inches. The dotted line is the power to weight ratio derivative at the same conditions. Figure 33 shows that the cut-off ratio increasing linearly until 2.5 and then behaves parabolic. The optimal cut-off ratio for highest power to weight ratio is 2.75.

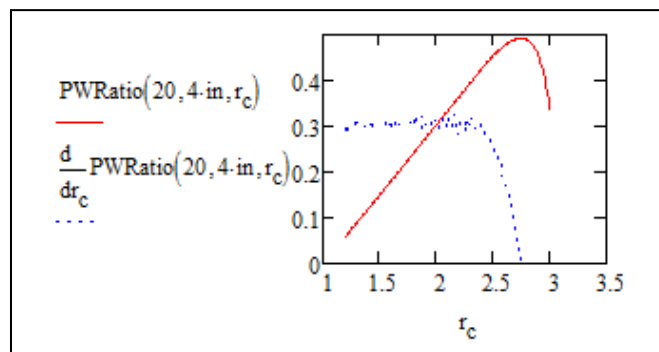


Figure 33: Power to Weight Ratio as a Function of Cut-Off Ratio

The compression ratio on a diesel engine typically ranges from 14 to 24 (Engineers Edge, 2012). Figure 34 demonstrates how the power to weight ratio varies with the compression ratio. The line occurs at a cut-off ratio of 2.75 and a bore of 4 inches. The power to weight ratio reaches a maximum of 0.492 at a compression ratio of approximately 20. This figure demonstrates that increasing the compression ratio will increase the power to weight ratio, until the relative maximum for a specified cut-off ratio is achieved.

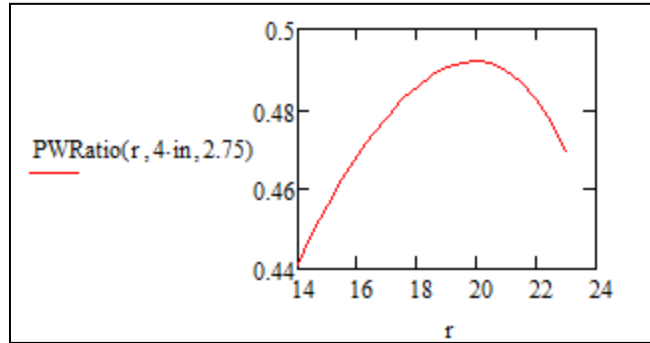


Figure 34: Power to Weight Ratio as a Function of Compression Ratio

Similarly to the gasoline engine, the range of bore sizes on a diesel NorEaster engine varies from 3 to 5 inches. Figure 35 demonstrates how the power to weight ratio varies with bore size. The line occurs at a cut-off ratio of 2.75 and a compression ratio of 20. With our weight estimates, a power to weight ratio of 0.49 can be achieved at a bore of approximately 4 inches. This graph shows that by increasing the bore size within the range of 3 in to 5 in, a higher power to weight ratio can be achieved.

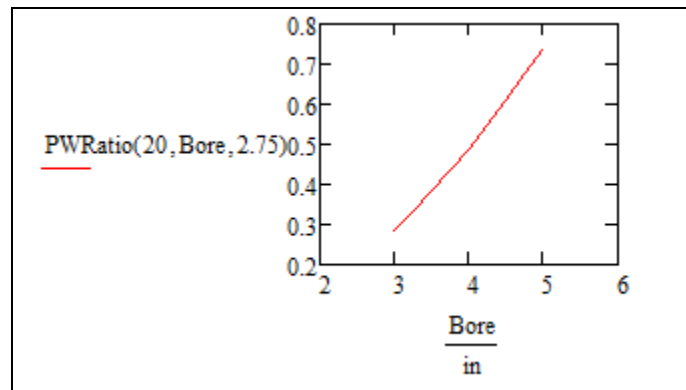


Figure 35: Power to Weight Ratio as a Function of Bore Size

As with the gasoline engine, the weight of the diesel engine is dependent upon the bore. Figure 31 in Section 4.1 demonstrates the calculation that was used to obtain the weight.

### 4.3 Overall Findings for the NorEaster Engine Designs

The weights calculated in Sections 4.1 and 4.2 used a safety factor of 2 for most of the components. The lowest safety factor was 1.5. This results in a conservative weight estimate and a lower power to weight ratio than with a lower safety factor. Typically, aircraft have a safety factor of 1.5 (Acar et al., 2004). Table 8 is a table comparing the different weights and power to weight ratios that can be calculated for both gasoline and diesel engines at varying various engine design parameters. Table 8 provides a summary of these values. Out of the four NorEaster engine configurations shown below, the best power to weight ratio is the 4 inch bore diesel engine. This will give a power to weight ratio of 0.49.

	Fire Scout	NorEaster Diesel		NorEaster Gasoline	
		3 in Bore	4 in Bore	3 in Bore	4 in Bore
<b>Engine Weight (lb)</b>	173	812	842.5	812	842.5
<b>Power (hp)</b>	419.7	233	414	218.2	388
<b>Power to Weight</b>	2.43	0.29	0.49	0.27	0.46

**Table 8: Comparison of the Power to Weight Ratios at Different Weight and Engine Parameters**

Table 8 also demonstrates the vast differences in the power to weight of the Fire Scout turbine engine to the NorEaster engine. The Fire Scout has a power to weight ratio of 2.43. However, this power to weight ratio does not include the weight of the transmission, gearing, or tail rotor. These components would not be needed in the NorEaster engine design. Therefore, comparing these two values is misleading.

Table 9 shows both the power to weight of the Fire Scout at its minimum and maximum weight. These two values are 0.2 and 0.13 respectively, which are significantly less than the power to weight of the engine shown in Table 8. Additional weight of the NorEaster can be attributed to the specific needs of the consumer. To have a better power to weight ratio (horse power divided by total helicopter weight) than the current Fire Scout, the NorEaster’s total weight would need to be under 2045 pounds. Since the engine would weigh just under 900 pounds, the additional components would need to be less than 1145 pounds. Because the

NorEaster does not require a tail rotor, transmission or gearing, it is difficult to compare the Fire Scout and the NorEaster without all of Sikorsky's information.

<b>Fire Scout</b>	
Empty Weight (lb)	2073
Power to Empty Weight of Fire Scout	0.2
Max Takeoff Weight (lb)	3150
Power to Max Takeoff Weight of Fire Scout	0.13

**Table 9: Fire Scout Power to Weight**

## 5.0 Conclusions and Recommendations

The goal of this project was to model the thermodynamic behavior of the NorEaster engine, calculate the power to weight ratio, and assess its future development possibilities. In order to perform this calculation, we developed two mathematical models using Mathcad, one for a diesel engine design and one for a gasoline engine design. Both of these models use air-standard Otto Cycle analysis to calculate the engine's output power and then divide that value by the weight, which was calculated by the NorEaster Design team.

In order to generate these models, we studied the existing prototype of the NorEaster engine. First, the team analyzed the rotor blades used on the engine. These blades resemble the NACA0015 airfoils used on aircraft. They are appropriate because they will minimize engine stalls, and they will help maximize the revolutions per minute.

To further assess the existing NorEaster engine prototype, we performed a dynamometer test and a pressure test. Unfortunately, these test results showed that there are several problems and inefficiencies in the prototype. During these tests, we encountered problems due to leaks and the fact that only one cylinder was regularly firing. While the output power does increase with rpm, it was not as large an increase as expected. Additionally, the motoring pressure in the cylinder heads was lower than anticipated. We do not yet have any ample explanation for these discrepancies in data, but believe that some of them can be attributed to the flaws in the prototype.

Despite these flaws in the prototype, the team analyzed new designs of the NorEaster engine. These new designs need to meet the United States Military's desired power to weight ratio of 0.5. The Design Team's NorEaster engine with a 4 inch bore and gasoline fuel generates a power to weight ratio of 0.46. The same engine running on diesel fuel generates a power to weight of 0.49. Both of these designs utilize a 2.0 safety factor for most components. The lowest safety factor in the design is 1.5. The materials selections and safety factor of the engine could be altered to reduce the weight and thus increase the power to weight ratio. From our calculated power, we determined that the NorEaster weight would need to be reduced by approximately 15 pounds in order to achieve a power to weight of 0.5. Therefore, we recommend building a larger

prototype of the engine with a lower safety factor and ideal engine parameters. This new prototype could be tested and compared to our mathematical model's power estimates.

Since the NorEaster engine does not utilize a tail rotor, transmission or gears, we also recommend obtaining the weight of these components for Sikorsky's current Fire Scout. This information will give a clear representation of the advantages and disadvantages of the NorEaster engine and allow us to better compare the two aircraft.

## 6.0 References

- Acar, E., Haftka, R.T. and Kale, A. (2004) "Effects of Error, Variability, Testing and Safety Factors on Aircraft Safety." Department of Mechanical and Aerospace Engineering, University of Florida: Florida Accessed March 22, 2012. [http://savannah.gatech.edu/workshop/rec04/proceedings/papers/Acar\\_effects\\_of\\_error.pdf](http://savannah.gatech.edu/workshop/rec04/proceedings/papers/Acar_effects_of_error.pdf)
- CSEE. "NACA 0015." UMBC: Maryland. Accessed April 25, 2012. [http://www.csee.umbc.edu/~squire/cs455\\_lairfoil.shtml](http://www.csee.umbc.edu/~squire/cs455_lairfoil.shtml)
- Drela, Mark. (2001) "X-Foil 6.94." MIT Software and Programming. Accessed October 6, 2011. <http://web.mit.edu/drela/Public/web/xfoil/>
- Dyno Simulation Software. (2007) "Virtual Engine Software." Challenger Engine Software. Accessed October 2, 2011. <http://www.virtualengine2000.com/Calculator.htm>
- Engineering Software. "Diesel Cycle Analysis." Engineering-4e. Germantown, MD. Accessed February 23, 2012. <http://www.engineering-4e.com/diesel.pdf>
- Engineers Edge. (2012) "Diesel Engine Construction and Operation." Engineers Edge, LLC: Solutions By Design. Accessed February 23, 2012. [http://www.engineersedge.com/power\\_transmission/diesel\\_engine.htm](http://www.engineersedge.com/power_transmission/diesel_engine.htm)
- Glenn Research Center. (2008) "Ideal Otto Cycle." NASA. Accessed October 5, 2011. <http://wright.nasa.gov/airplane/otto.html>
- Gotoh, T. and Motoyama, Y. "The Effect of Higher Compression Ratio in Two-Stroke Engines." Yamaha motor Co, Ltd. Accessed February 23, 2012. [http://www.drrinc.com/pdfs/higher\\_compression6.pdf](http://www.drrinc.com/pdfs/higher_compression6.pdf)
- Heywood, John. (1988) "Internal Combustion Engine Fundamentals." McGraw-Hill Book Company: New York
- Loeffler, K. (2003) "Internal Combustion Engine." Explore Cornell. Accessed October 5, 2011. [http://ecommons2.library.cornell.edu/web\\_archive/explore.cornell.edu/scenedd12.h](http://ecommons2.library.cornell.edu/web_archive/explore.cornell.edu/scenedd12.h)



tml?scene=Digital%20Library%20of%20Kinematics&stop=DLK%20-%20Gallery&view=DLK%20-%20Gallery%2006

MIT: Massachusetts Institute of Technology. (2006) "Thermodynamics and Propulsion." Accessed December 7, 2011. <http://web.mit.edu/16.unified/www/SPRING/propulsion/notes/node25.html>

Military Factory. (2010) "General Atomics MQ-1/RQ-1 Predator (Predator A) Unmanned Aerial Vehicle." Accessed November 10, 2011. [http://www.militaryfactory.com/aircraft/detail.asp?aircraft\\_id=46](http://www.militaryfactory.com/aircraft/detail.asp?aircraft_id=46)

Moran, M. and Shapiro, H. (2011) "Fundamentals of Engineering Thermodynamics." 7<sup>th</sup> Edition. John Wiley & Sons, Inc: United States of America.

Northrop Grumman. (2011). "MQ-8B Fire Scout." Accessed November 7, 2011. [http://www.as.northropgrumman.com/products/mq8bfirescout\\_navy/index.html](http://www.as.northropgrumman.com/products/mq8bfirescout_navy/index.html)

O'Neill, James. (2007) U.S. Patent No. 7,219,631 B1. "High Torque, Low Velocity, Internal Combustion Engine."

Office of Energy Efficiency and Renewable Energy. (2003) "Just the Basics: Diesel Engine." U.S. Department of Energy. Accessed February 23, 2012. [http://www1.eere.energy.gov/vehiclesandfuels/pdfs/basics/jtb\\_diesel\\_engine.pdf](http://www1.eere.energy.gov/vehiclesandfuels/pdfs/basics/jtb_diesel_engine.pdf)

Ricardo. (2011) "Engine Performance." Ricardo Software. Accessed October 2, 2011. <http://www.ricardo.com/en-gb/What-we-do/Software/Products/WAVE/EnginePerformance/>

Scott, Jeff. (2001) "Helicopter Lift Equation." Accessed December 8, 2011. <http://www.aerospaceweb.org/question/aerodynamics/q0037.shtml>

Sikorsky. (2011) "Product Innovation: X2 Technology Demonstrator." United Technologies Company. Accessed November 13, 2011. <http://www.sikorsky.com/Innovation/Vision+of+the+future/Technologies/X2+Technology>

Stone, Richard. (1999) "Introduction to Internal Combustion Engines." 3<sup>rd</sup> Edition. Society of Automotive Engineers, Inc.: Great Britain.

Taylor, Charles. (1985). "The Internal Combustion Engine in Theory and in Practice. "Volume 1. The M.I.T. Press. Cambridge, MA.

Taylor, Charles. (1985). "The Internal Combustion Engine in Theory and in Practice. "Volume 2. The M.I.T. Press. Cambridge, MA.

UAV Engines LTD. (2004) "AR741-38 BHP – For Small Surveillance UAVs" UAV Engines LTD: United Kingdom. Accessed October 1, 2011.  
<http://www.uavenginesltd.co.uk/index.php?id=397>

## Appendix A – Blade to Engine Relationships

ss = sound of sound  
 sf = safety factor  
 rav = rotor angular velocity  
 l = rotor length  
 rs = rotor speed at tip  
 spl = speed limit  
 mxsp = max speed

Variable

$$sf := 1.2$$

$$l := 3\text{m}$$

$$spl := \left( \frac{ss}{sf} \right) - mxsp = 334.339\text{-mph}$$

Known

$$ss := 340.29 \frac{\text{m}}{\text{s}} = 761.207\text{-mph}$$

$$mxsp := 300\text{mph}$$

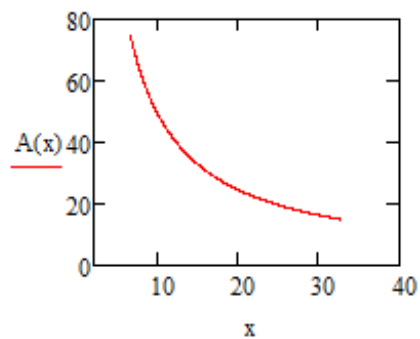
$$rav := \frac{spl}{l} = 475.756 \frac{\text{rev}}{\text{min}} \quad A(x) := \frac{spl}{x}$$

$$rs := rav \cdot l = 334.339\text{-mph}$$

If rav = 500

$$rav := 500 \frac{\text{rev}}{\text{min}}$$

$$rs := rav \cdot l = 351.377\text{-mph}$$



## Appendix B – Dynamometer Mathcad

### Dynamometer Test 1 Calculations and Results

**Dynamometer Test Results**

RPM	Horsepower	
$X := \begin{pmatrix} 1050 & 1 \\ 600 & 1 \\ 500 & 1 \\ 760 & 1 \end{pmatrix}$	$Y := \begin{pmatrix} 0.68 \\ 5 \\ 1.87 \\ 1.67 \end{pmatrix}$	$N := 3$  $i := 0, 1..N$

**Linear Regression Computation**

$$A := X^T \cdot Y$$
$$M := X^T X$$
$$A = \begin{pmatrix} 5.918 \times 10^3 \\ 9.22 \end{pmatrix}$$
$$M = \begin{pmatrix} 2.29 \times 10^6 & 2.91 \times 10^3 \\ 2.91 \times 10^3 & 4 \end{pmatrix}$$
$$M^{-1} = \begin{pmatrix} 5.778 \times 10^{-6} & -4.203 \times 10^{-3} \\ -4.203 \times 10^{-3} & 3.308 \end{pmatrix}$$
$$u := M^{-1} \cdot A$$
$$u = \begin{pmatrix} -4.561 \times 10^{-3} \\ 5.623 \end{pmatrix}$$
$$y(x) := u_0 \cdot x + u_1$$

$$y_{e_i} := u_0 \cdot X_{i,0} + u_1$$

$$SS_{err} := \sum_{i=0}^N (Y_i - y_{e_i})^2$$

SSerr = 6.896

$$Y_{mean} := \frac{1}{(N+1)} \cdot \sum_{i=0}^N Y_i$$

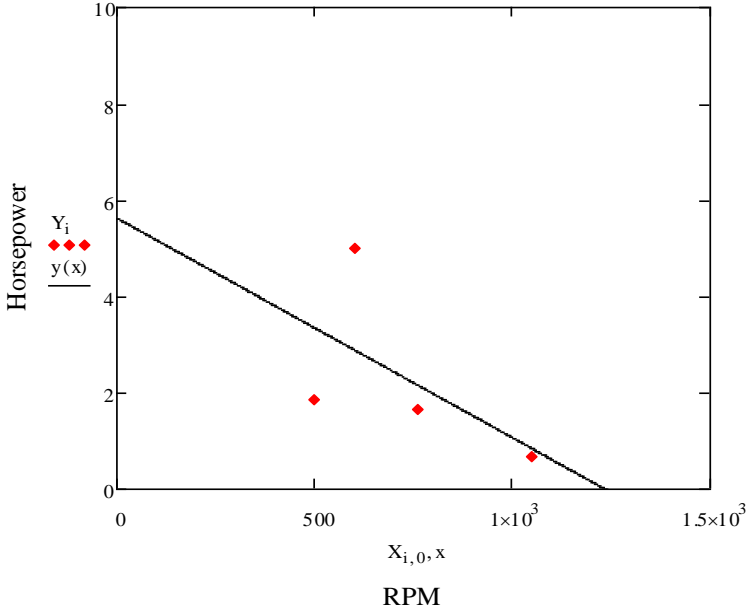
$$SS_{tot} := \sum_{i=0}^N (Y_i - Y_{mean})^2 \qquad SS_{tot} = 10.496$$

$$R := \sqrt{1 - \frac{SS_{err}}{SS_{tot}}}$$

R = 0.586

$$R^2 = 0.343$$

Dynamometer Test Results



## Dynamometer Test 2 Calculations and Results

### Dynamometer Test Results

RPM	Horsepower	
$X := \begin{pmatrix} .9 & 1 \\ .8 & 1 \\ 1.2 & 1 \\ 1 & 1 \\ 1 & 1 \\ 1.2 & 1 \\ 1.1 & 1 \\ 1.1 & 1 \end{pmatrix}$	$Y := \begin{pmatrix} .938715 \\ .952126 \\ 1.166689 \\ 1.072818 \\ 1.086228 \\ 1.086228 \\ .978946 \\ 1.005767 \end{pmatrix}$	$N := 7$ $i := 0, 1..N$

### Linear Regression Computation

$$\underline{A} := X^T \cdot Y$$

$$M := X^T X$$

$$A = \begin{pmatrix} 8.652 \\ 8.288 \end{pmatrix}$$

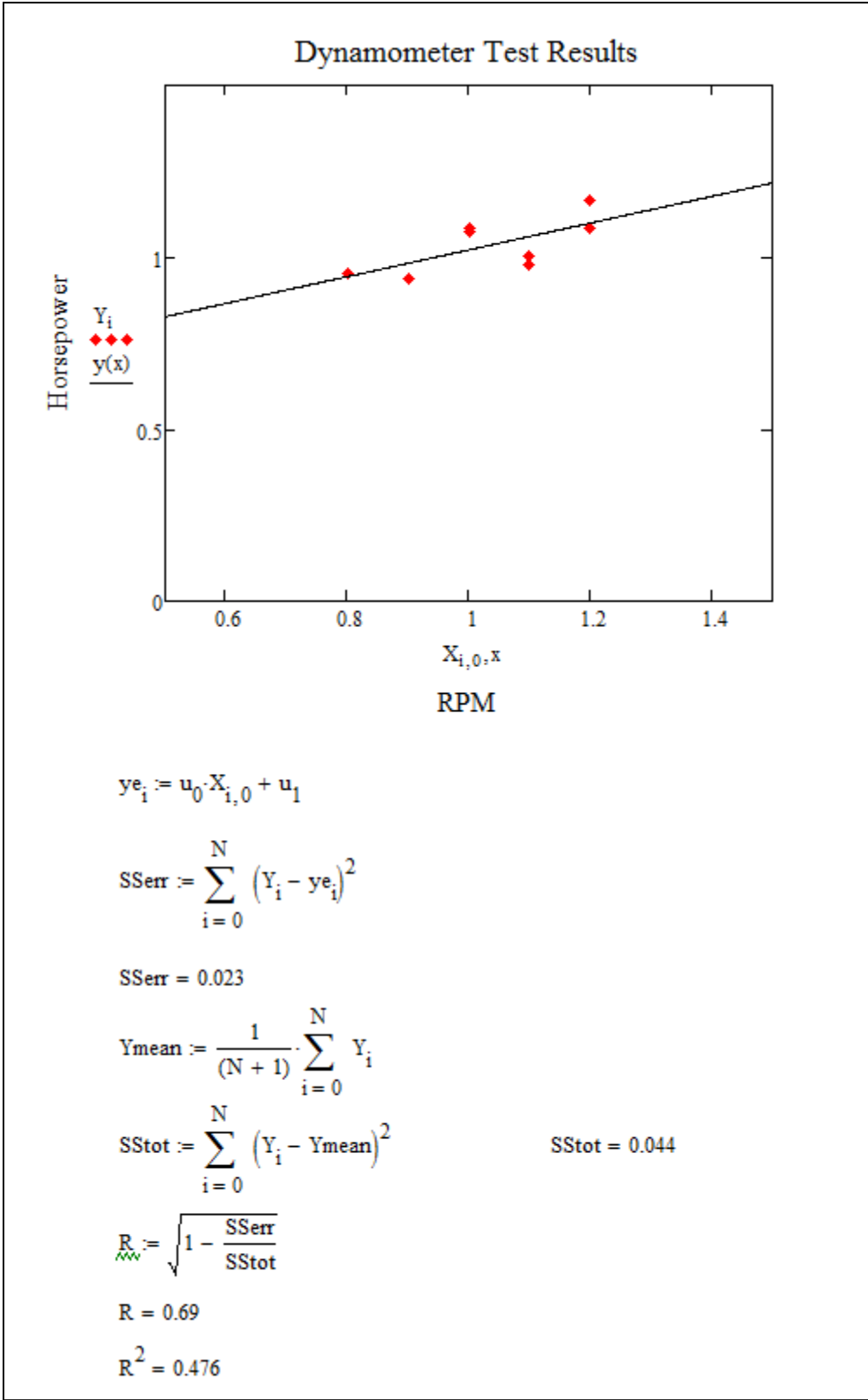
$$M = \begin{pmatrix} 8.75 & 8.3 \\ 8.3 & 8 \end{pmatrix}$$

$$M^{-1} = \begin{pmatrix} 7.207 & -7.477 \\ -7.477 & 7.883 \end{pmatrix}$$

$$u := M^{-1} \cdot A$$

$$u = \begin{pmatrix} 0.389 \\ 0.632 \end{pmatrix}$$

$$y(x) := u_0 \cdot x + u_1$$



## Appendix C – Gasoline and Diesel Mathematical Models

### Gasoline Engine Model

200	142.56	1707	1.864	2250
210	149.69	1512	2.012	2200
220	156.82	1346	2.175	2150
230	164	1205	2.35	2100
240	171.13	1084	2.555	2050
250	178.28	979	2.776	2000
260	185.45	887.8	3.022	1950
270	192.6	808	3.295	1900
280	199.75	738	3.601	1850
285	203.33	706.1	3.944	1800
290	206.91	676.1	4.328	1750
295	210.49	647.9	4.761	1700
300	214.07	621.2	4.949	1680
305	217.67	596	5.147	1660
310	221.25	572.3	5.355	1640
315	224.85	549.8	5.574	1620
320	228.42	528.6	5.804	1600
325	232.02	508.4	6.046	1580
330	235.61	489.4	6.301	1560
340	242.82	454.1	6.569	1540
350	250.02	422.2	6.854	1520
360	257.24	393.4	7.152	1500
370	264.46	367.2	7.468	1480
380	271.69	343.4	7.801	1460
390	278.93	321.5	8.153	1440
400	286.16	301.6	8.526	1420
410	293.43	283.3	8.919	1400
420	300.69	266.6	9.337	1380
430	307.99	251.1	9.78	1360
440	315.3	236.8	10.247	1340
450	322.62	223.6	10.747	1320
460	329.97	211.4	11.275	1300
470	337.32	200.1	11.835	1280
480	344.7	189.5	12.435	1260
490	352.08	179.7	13.069	1240
500	359.49	170.6	13.747	1220



	510	366.92	162.1		14.47	1200
	520	374.36	154.1		15.241	1180
	530	381.84	146.7		16.064	1160
	540	389.34	139.7		16.946	1140
	550	396.86	133.1		17.886	1120
	560	404.42	127		18.896	1100
	570	411.97	121.2		19.98	1080
	580	419.55	115.7		21.14	1060
	590	427.15	110.6		22.39	1040
	600	434.78	105.8		23.72	1020
	610	442.42	101.2		25.17	1000
	620	450.09	96.92		26.73	980
	630	457.78	92.84		28.4	960
	640	465.5	88.99		30.22	940
	650	473.25	85.34		32.18	920
	660	481.01	81.89		34.31	900
	670	488.81	78.61		36.61	880
	680	496.62	75.5		39.12	860
	690	504.45	72.56		41.85	840
	700	512.33	69.76		44.84	820
	710	520.23	67.07		48.08	800
	720	528.14	64.53		49.86	790
	730	536.07	62.13		51.64	780
	740	544.02	59.82		53.39	770
	750	551.99	57.63		55.54	760
$T_{uv} :=$	760	560.01	55.54	$V_T :=$	57.63	750
	770	568.07	53.39		59.82	740
	780	576.12	51.64		62.13	730
	790	584.21	49.86		64.53	720
	800	592.3	48.08		67.07	710
	820	608.59	44.84		69.76	700
	840	624.95	41.85		72.56	690
	860	641.4	39.12		75.5	680
	880	657.95	36.61		78.61	670
	900	674.58	34.31		81.89	660
	920	691.28	32.18		85.34	650

940	708.08	30.22	88.99	640
960	725.02	28.4	92.84	630
980	741.98	26.73	96.92	620
1000	758.94	25.17	101.2	610
1020	776.1	23.72	105.8	600
1040	793.36	22.39	110.6	590
1060	810.62	21.14	115.7	580
1080	827.88	19.98	121.2	570
1100	845.33	18.896	127	560
1120	862.79	17.886	133.1	550
1140	880.35	16.946	139.7	540
1160	897.91	16.064	146.7	530
1180	915.57	15.241	154.1	520
1200	933.33	14.47	162.1	510
1220	951.09	13.747	170.6	500
1240	968.95	13.069	179.7	490
1260	986.9	12.435	189.5	480
1280	1004.76	11.835	200.1	470
1300	1022.82	11.275	211.4	460
1320	1040.88	10.747	223.6	450
1340	1058.94	10.247	236.8	440
1360	1077.1	9.78	251.1	430
1380	1095.26	9.337	266.6	420
1400	1113.52	8.919	283.3	410
1420	1131.77	8.526	301.6	400
1440	1150.13	8.153	321.5	390
1460	1168.49	7.801	343.4	380
1480	1186.95	7.468	367.2	370
1500	1205.41	7.152	393.4	360
1520	1223.87	6.854	422.2	350
1540	1242.43	6.569	454.1	340
1560	1260.99	6.301	489.4	330
1580	1279.65	6.046	508.4	325
1600	1298.3	5.804	528.6	320
1620	1316.96	5.574	549.8	315
1640	1335.72	5.355	572.3	310

1660	1354.48	5.147			596	305
1680	1373.24	4.949			621.2	300
1700	1392.7	4.761			647.9	295
1750	1439.8	4.328			676.1	290
1800	1487.2	3.944			706.1	285
1850	1534.9	3.601			738	280
1900	1582.6	3.295			808	270
1950	1630.6	3.022			887.8	260
2000	1678.7	2.776			979	250
2050	1726.8	2.555			1084	240
2100	1775.3	2.35	$T_m := T_{uv}^{(0)} \cdot K$	$T_v := V_T^{(0)} \cdot K$	1205	230
2150	1823.8	2.175	$U_m := T_{uv}^{(1)}$		1346	220
2200	1872.4	2.012		$v_v := V_T^{(1)}$	1512	210
2250	1921.3	1.864	$v_m := T_{uv}^{(2)}$		1707	200

## Air Standard Otto Cycle Analysis for BMW Design (pg 500)

$$r := 6,65..14$$

$$f(r) := r \quad r = \text{Compression Ratio } V(1)/V(2)$$

$$\underline{R} := 287 \cdot \frac{\text{J}}{\text{kg} \cdot \text{K}} \quad R = \text{Universal Gas Constant for Air}$$

### First Step of the Otto Cycle

$$\text{Bore} := 3\text{in}, 3.25\text{in}..5\text{in} \quad \text{Stroke} := 3\text{in}$$

$$V_1(r, \text{Bore}) := \text{Stroke} \cdot \pi \cdot \left(\frac{\text{Bore}}{2}\right)^2 \cdot \left(1 + \frac{1}{1 - \frac{1}{r}}\right)$$

$$T_1 := 300 \cdot \text{K} \quad T(1) = \text{Known Temperature}$$

$$p_1 := 101.3\text{kPa} \quad p(1) = \text{Known Atmospheric Pressure}$$

$$v_{r1} := \text{linterp}(T_m, v_m, T_1) = 621.2$$

### Second Step of the Otto Cycle

$$v_{r2}(r) := \frac{v_{r1}}{r} \quad +$$

$$T_2(r) := \text{linterp}(T_v, v_v, v_{r2}(r) \cdot \text{K}) \cdot \text{K}$$

$$p_2(r) := p_1 \cdot \left(\frac{T_2(r)}{T_1}\right)(r)$$

$$p_2 = f(\text{Unitless}) \rightarrow \text{Pressure}$$

### Third Step of the Otto Cycle

$x := 1500\text{K}, 1510\text{K} \dots 2250\text{K}$   $T(3) = \text{Known Temperature}$

$$T_3(x) := x$$
$$v_{r3}(x) := \text{linterp}(T_m, v_m, T_3(x))$$

$$p_3(x, r) := p_2(r) \cdot \left( \frac{T_3(x)}{T_2(r)} \right)$$

$$p_3 = f(\text{any1}, \text{Unitless}) \rightarrow \text{any1} \cdot \text{Mass} \cdot \text{Time}^{-2} \cdot \text{Temperature}^{-1} \cdot \text{Length}^{-1}$$

### Fourth Step of the Otto Cycle

$$v_{r4}(x, r) := v_{r3}(x) \cdot (r)$$

$$v_{r4} = f(\text{Temperature}, \text{any1}) \rightarrow \text{any1}$$

$$T_4(x, r) := \text{linterp}(T_v, v_v, v_{r4}(x, r) \cdot K) \cdot K$$

$$p_4(x, r) := p_1 \cdot \left( \frac{T_4(x, r)}{T_1} \right)$$

$$p_4 = f(\text{Temperature}, \text{Unitless}) \rightarrow \text{Pressure}$$

### Overall Engine

$$m(r, \text{Bore}) := \frac{(p_1 \cdot V_1(r, \text{Bore}))}{R \cdot T_1}$$

$$m = f(\text{Unitless}, \text{any1}) \rightarrow \text{any1}^2 \cdot \text{Mass} \cdot \text{Length}^{-2}$$

### Find Internal Energy (u) at each Temperature

$$u_1 := \text{linterp}(T_m, U_m, T_1) = 214.07$$

$$u_2(r) := \text{linterp}(T_m, U_m, T_2(r))$$

$$u_3(x) := \text{linterp}(T_m, U_m, T_3(x))$$

$$u_4(x, r) := \text{linterp}(T_m, U_m, T_4(x, r))$$

## Work Analysis

$$W_{\text{cyc}}(x, r, \text{Bore}) := m(r, \text{Bore}) \cdot (u_3(x) - u_4(x, r) - u_2(r) + u_1) \cdot 1000 \frac{\text{J}}{\text{kg}}$$

$$W_{\text{cyc}} = f(\text{Temperature, Unitless, any1}) \rightarrow \text{any1}^2 \cdot \text{Mass} \cdot \text{Time}^{-2}$$

## Ideal Individual Cylinder Head Power Analysis

$$\text{IdealP}(x, r, \text{Bore}) := W_{\text{cyc}}(x, r, \text{Bore}) \cdot 1200 \cdot \text{rpm}$$

$$\text{IdealP} = f(\text{Temperature, Unitless, any1}) \rightarrow \text{any1}^2 \cdot \text{Mass} \cdot \text{Time}^{-3}$$

$$\text{IdealP} = \bullet \cdot \text{hp}$$

## Actual Individual Cylinder Head Power Analysis

$$n := 0.3 \quad n = \text{Engine Efficiency}$$

$$\text{ActualP}(x, r, \text{Bore}) := \text{IdealP}(x, r, \text{Bore}) \cdot (n)$$

$$\text{ActualP} = f(\text{Temperature, Unitless, any1}) \rightarrow \text{any1}^2 \cdot \text{Mass} \cdot \text{Time}^{-3}$$

$$\text{ActualP} = \bullet \cdot \text{hp}$$

## Overall Actual Power Analysis for 8 Cylinder Engine Design

$$\text{cyl} := 8 \quad \text{cyl} = \text{Number of Cylinder Heads}$$

$$\text{TotalActualP}_8(x, r, \text{Bore}) := \text{ActualP}(x, r, \text{Bore}) \cdot \text{cyl}$$

$$\text{TotalActualP}_8 = f(\text{Temperature, Unitless, any1}) \rightarrow \text{any1}^2 \cdot \text{Mass} \cdot \text{Time}^{-3}$$

$$\text{TotalActualP}_8 = \bullet \cdot \text{hp}$$

## Power to Weight Ratio

4

Thickness side  $t$ , Thickness top  $t_e$ , Length from black to top of chamber  $L$ , Bore  $B$ , density  $\rho$ ,

$$\rho := 7.8 \frac{\text{gm}}{\text{cm}^3} = 7.8 \times 10^3 \frac{\text{kg}}{\text{m}^3} \quad t := 0.5\text{in} \quad t_e := 0.75\text{in} \quad L := 12\text{in}$$

$$\text{Addition}_{\text{per.cylinder}}(\text{Bore}) := \rho \cdot \frac{\pi}{4} \cdot \left[ (\text{Bore} + 2t)^2 - \text{Bore}^2 \right] \cdot (L - t_e) + \left[ (\text{Bore} + 2t)^2 \cdot t_e \right]$$

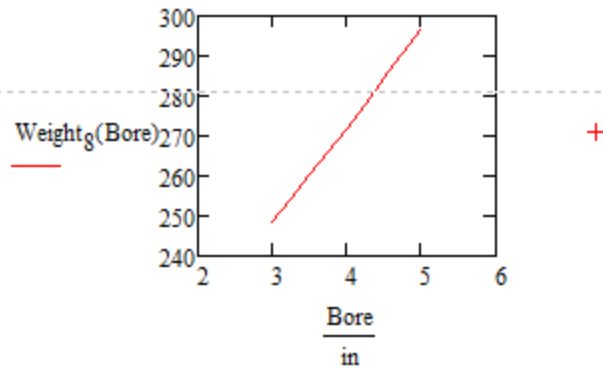
Known Weight at Known Bore

$$\text{Known}_{\text{weight}} := 600\text{lbm}$$

**Weight = Known Total Engine Weight**

$$\text{Known}_{\text{Bore}} := 4\text{in}$$

$$\text{Weight}_g(\text{Bore}) := \text{Known}_{\text{weight}} - 8 \cdot \text{Addition}_{\text{per.cylinder}}(\text{Known}_{\text{Bore}}) + 8 \cdot \text{Addition}_{\text{per.cylinder}}(\text{Bore})$$



$$\frac{\text{TotalActualP}_g(x, r, \text{Bore})}{\text{in}}$$

$$\text{PWRatio}_g(x, r, \text{Bore}) := \frac{\text{hp}}{\text{Weight}_g(\text{Bore})}$$

$$\text{PWRatio}_g = f(\text{Temperature, Unitless, Length}) \rightarrow \text{Unitless}$$

$$\text{PWRatio}_g(1800\text{-K}, 10, 4\text{-in}) = 0.544$$

## Diesel Engine Model

200	142.56	1707	1.864	2250
210	149.69	1512	2.012	2200
220	156.82	1346	2.175	2150
230	164	1205	2.35	2100
240	171.13	1084	2.555	2050
250	178.28	979	2.776	2000
260	185.45	887.8	3.022	1950
270	192.6	808	3.295	1900
280	199.75	738	3.601	1850
285	203.33	706.1	3.944	1800
290	206.91	676.1	4.328	1750
295	210.49	647.9	4.761	1700
300	214.07	621.2	4.949	1680
305	217.67	596	5.147	1660
310	221.25	572.3	5.355	1640
315	224.85	549.8	5.574	1620
320	228.42	528.6	5.804	1600
325	232.02	508.4	6.046	1580
330	235.61	489.4	6.301	1560
340	242.82	454.1	6.569	1540
350	250.02	422.2	6.854	1520
360	257.24	393.4	7.152	1500
370	264.46	367.2	7.468	1480
380	271.69	343.4	7.801	1460
390	278.93	321.5	8.153	1440
400	286.16	301.6	8.526	1420
410	293.43	283.3	8.919	1400
420	300.69	266.6	9.337	1380
430	307.99	251.1	9.78	1360
440	315.3	236.8	10.247	1340
450	322.62	223.6	10.747	1320
460	329.97	211.4	11.275	1300
470	337.32	200.1	11.835	1280
480	344.7	189.5	12.435	1260
490	352.08	179.7	13.069	1240



	490	352.08	179.7		13.069	1240
	500	359.49	170.6		13.747	1220
	510	366.92	162.1		14.47	1200
	520	374.36	154.1		15.241	1180
	530	381.84	146.7		16.064	1160
	540	389.34	139.7		16.946	1140
	550	396.86	133.1		17.886	1120
	560	404.42	127		18.896	1100
	570	411.97	121.2		19.98	1080
	580	419.55	115.7		21.14	1060
	590	427.15	110.6		22.39	1040
	600	434.78	105.8		23.72	1020
	610	442.42	101.2		25.17	1000
	620	450.09	96.92		26.73	980
	630	457.78	92.84		28.4	960
	640	465.5	88.99		30.22	940
	650	473.25	85.34		32.18	920
	660	481.01	81.89		34.31	900
	670	488.81	78.61		36.61	880
	680	496.62	75.5		39.12	860
	690	504.45	72.56		41.85	840
	700	512.33	69.76		44.84	820
	710	520.23	67.07		48.08	800
	720	528.14	64.53		49.86	790
	730	536.07	62.13		51.64	780
	740	544.02	59.82		53.39	770
	750	551.99	57.63		55.54	760
$T_{uv} :=$	760	560.01	55.54		57.63	750
	770	568.07	53.39		59.82	740
	780	576.12	51.64		62.13	730
	790	584.21	49.86		64.53	720
	800	592.3	48.08		67.07	710
	820	608.59	44.84		69.76	700
	840	624.95	41.85		72.56	690
	860	641.4	39.12		75.5	680
	880	657.95	36.61		78.61	670

$V_T :=$

880	657.95	36.61	78.61	670
900	674.58	34.31	81.89	660
920	691.28	32.18	85.34	650
940	708.08	30.22	88.99	640
960	725.02	28.4	92.84	630
980	741.98	26.73	96.92	620
1000	758.94	25.17	101.2	610
1020	776.1	23.72	105.8	600
1040	793.36	22.39	110.6	590
1060	810.62	21.14	115.7	580
1080	827.88	19.98	121.2	570
1100	845.33	18.896	127	560
1120	862.79	17.886	133.1	550
1140	880.35	16.946	139.7	540
1160	897.91	16.064	146.7	530
1180	915.57	15.241	154.1	520
1200	933.33	14.47	162.1	510
1220	951.09	13.747	170.6	500
1240	968.95	13.069	179.7	490
1260	986.9	12.435	189.5	480
1280	1004.76	11.835	200.1	470
1300	1022.82	11.275	211.4	460
1320	1040.88	10.747	223.6	450
1340	1058.94	10.247	236.8	440
1360	1077.1	9.78	251.1	430
1380	1095.26	9.337	266.6	420
1400	1113.52	8.919	283.3	410
1420	1131.77	8.526	301.6	400
1440	1150.13	8.153	321.5	390
1460	1168.49	7.801	343.4	380
1480	1186.95	7.468	367.2	370
1500	1205.41	7.152	393.4	360
1520	1223.87	6.854	422.2	350
1540	1242.43	6.569	454.1	340
1560	1260.99	6.301	489.4	330
1580	1279.65	6.046	508.4	325
1600	1298.3	5.804	528.6	320

1620	1316.96	5.574
1640	1335.72	5.355
1660	1354.48	5.147
1680	1373.24	4.949
1700	1392.7	4.761
1750	1439.8	4.328
1800	1487.2	3.944
1850	1534.9	3.601
1900	1582.6	3.295
1950	1630.6	3.022
2000	1678.7	2.776
2050	1726.8	2.555
2100	1775.3	2.35
2150	1823.8	2.175
2200	1872.4	2.012
2250	1921.3	1.864

549.8	315
572.3	310
596	305
621.2	300
647.9	295
676.1	290
706.1	285
738	280
808	270
887.8	260
979	250
1084	240
1205	230
1346	220
1512	210
1707	200

$$T_m := T_{uv}^{(0)} \cdot K \quad T_v := V_T^{(0)} \cdot K$$

$$U_m := T_{uv}^{(1)} \quad v_v := V_T^{(1)}$$

$$v_m := T_{uv}^{(2)}$$

## Air Standard Diesel Cycle Analysis (pg 504)

$$r := 14, 14.5.. 23 \quad r = \text{Compression Ratio } V(1)/V(2)$$

$$\frac{R}{M} := 287 \cdot \frac{\text{J}}{\text{kg} \cdot \text{K}} \quad R = \text{Universal Gas Constant for Air}$$

$$r_c := 1.2, 1.21.. 3 \quad r(c) = \text{cut-off ratio, which is } V(3)/V(2)$$

**First Step of the Diesel Cycle**      Bore := 3in, 3.25in.. 5.5in      Stroke := 3in

$$V_1(r, \text{Bore}) := \text{Stroke} \cdot \pi \cdot \left( \frac{\text{Bore}}{2} \right)^2 \cdot \left( \frac{1}{1 - \frac{1}{r}} \right)$$

$$T_1 := 300\text{-K} \quad T(1) = \text{Known Temperature}$$

$$p_1 := 101.3\text{kPa} \quad p(1) = \text{Known Atmospheric Pressure}$$

$$v_{r1} := \text{linterp}(T_m, v_m, T_1) = 621.2$$

**Second Step of the Diesel Cycle**

$$v_{r2}(r) := \frac{v_{r1}}{r}$$

$$T_2(r) := \text{linterp}(T_v, v_v, v_{r2}(r) \cdot \text{K}) \cdot \text{K}$$

$$p_2(r) := p_1 \cdot \left( \frac{T_2(r)}{T_1} \right) (r)$$

### Third Step of the Diesel Cycle

$$T_3(r, r_c) := r_c T_2(r)$$

$$T_3 = f(\text{Unitless}, \text{any1}) \rightarrow \text{any1} \cdot \text{Temperature}$$

$$p_3(r, r_c) := p_2(r) \cdot \left( \frac{T_3(r, r_c)}{T_2(r)} \right)$$

$$p_3 = f(\text{Unitless}, \text{any1}) \rightarrow \text{any1} \cdot \text{Pressure}$$

$$v_{r3}(r, r_c) := \text{linterp}(T_m, v_m, T_3(r, r_c))$$

### Fourth Step of the Diesel Cycle

$$v_{r4}(r, r_c) := v_{r3}(r, r_c) \cdot (r)$$

$$v_{r4} = f(\text{Unitless}, \text{Unitless}) \rightarrow \text{Unitless}$$

$$T_4(r, r_c) := \text{linterp}[T_v, v_v, (v_{r4}(r, r_c)) \cdot K] \cdot K$$

$$p_4(r, r_c) := p_1 \cdot \left( \frac{T_4(r, r_c)}{T_1} \right)$$

$$p_4 = f(\text{Unitless}, \text{Unitless}) \rightarrow \text{Pressure}$$

### Overall Engine

$$\underline{m}(r, \text{Bore}) := \frac{(p_1 \cdot V_1(r, \text{Bore}))}{R \cdot T_1}$$

$$m = f(\text{Unitless}, \text{any1}) \rightarrow \text{any1}^2 \cdot \text{Mass} \cdot \text{Length}^{-2}$$

### Find Internal Energy (u) at each Temperature

$$\text{kJ} := 1000\text{J}$$

$$u_1 := \text{linterp}(T_m, U_m, T_1) \cdot \frac{\text{kJ}}{\text{kg}} = 214.07 \cdot \frac{\text{kJ}}{\text{kg}} \quad u_3(r, r_c) := \text{linterp}(T_m, U_m, T_3(r, r_c)) \cdot \frac{\text{kJ}}{\text{kg}}$$

$$u_2(r) := \text{linterp}(T_m, U_m, T_2(r)) \cdot \frac{\text{kJ}}{\text{kg}} \quad u_4(r, r_c) := \text{linterp}(T_m, U_m, T_4(r, r_c)) \cdot \frac{\text{kJ}}{\text{kg}}$$

### Work Analysis

$$W_{cyc}(r, Bore, r_c) := m(r, Bore) \cdot (u_3(r, r_c) - u_4(r, r_c) - u_2(r) + u_1)$$

$$W_{cyc} = f(\text{Unitless}, \text{any1}, \text{Unitless}) \rightarrow \text{any1}^2 \cdot \text{Mass} \cdot \text{Time}^{-2}$$

### Ideal Individual Cylinder Head Power Analysis

$$\text{IdealP}(r, Bore, r_c) := W_{cyc}(r, Bore, r_c) \cdot 1200 \cdot \text{rpm}$$

$$\text{IdealP} = f(\text{Unitless}, \text{any1}, \text{Unitless}) \rightarrow \text{any1}^2 \cdot \text{Mass} \cdot \text{Time}^{-3}$$

$$\text{IdealP} = \bullet \cdot \text{hp}$$

### Actual Individual Cylinder Head Power Analysis

$$n := 0.45 \quad n = \text{Engine Efficiency}$$

$$\text{ActualP}(r, Bore, r_c) := \text{IdealP}(r, Bore, r_c) \cdot (n)$$

$$\text{ActualP} = f(\text{Unitless}, \text{any1}, \text{Unitless}) \rightarrow \text{any1}^2 \cdot \text{Mass} \cdot \text{Time}^{-3}$$

$$\text{ActualP} = \bullet \cdot \text{hp} \quad \text{ActualP}(20, 5\text{-in}, 2) = 49.857 \cdot \text{hp}$$

### Overall Actual Power Analysis

$$\text{cyl} := 8 \quad \text{cyl} = \text{Number of Cylinder Heads}$$

$$\text{TotalActualP}(r, Bore, r_c) := \text{ActualP}(r, Bore, r_c) \cdot 8$$

$$\text{TotalActualP} = f(\text{Unitless}, \text{any1}, \text{Unitless}) \rightarrow \text{any1}^2 \cdot \text{Mass} \cdot \text{Time}^{-3}$$

$$\text{TotalActualP} = \bullet \cdot \text{hp} \quad \text{TotalActualP}(20, 5\text{in}, 2) = 398.852 \cdot \text{hp}$$

### Power to Weight Ratio

Thickness side  $t$ , Thickness top  $t_e$ , Length from black to top of chamber  $L$ , Bore  $B$ , density

$$t := 0.25\text{in}$$

$$t_e := 0.75\text{in}$$

Ask Jim to measure these

$$L := 15\text{in}$$

$$\rho := 7.8 \frac{\text{gm}}{\text{cm}^3} = 7.8 \times 10^3 \frac{\text{kg}}{\text{m}^3}$$

$$\text{Addition}_{\text{per.cylinder}}(\text{Bore}) := \rho \cdot \frac{\pi}{4} \cdot \left[ \left[ (\text{Bore} + 2t)^2 - \text{Bore}^2 \right] \cdot (L - t_e) + \left[ (\text{Bore} + 2t)^2 \cdot t_e \right] \right]$$

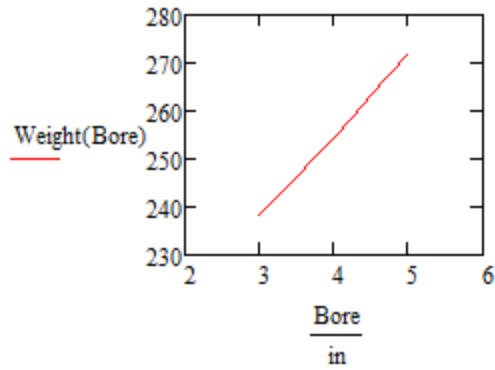
Known Weight at Known Bore

$$\text{Known}_{\text{weight}} := 600\text{lbm}$$

$$\text{Known}_{\text{Bore}} := 5\text{in}$$

Weight = Known Total Engine Weight

$$\text{Weight}(\text{Bore}) := \text{Known}_{\text{weight}} - 8 \cdot \text{Addition}_{\text{per.cylinder}}(\text{Known}_{\text{Bore}}) + 8 \cdot \text{Addition}_{\text{per.cylinder}}(\text{Bore})$$



Weight(5)

$$\text{PWRatio}(r, \text{Bore}, r_c) := \frac{\frac{\text{TotalActualP}(r, \text{Bore}, r_c)}{\text{hp}}}{\frac{\text{Weight}(\text{Bore})}{\text{lb}}}$$

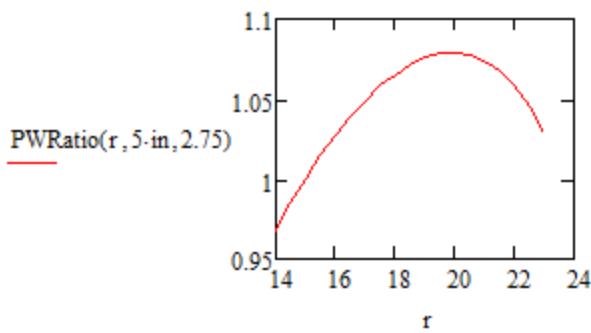
$$\text{PWRatio}(20, 5\text{-in}, 2.75) = 1.079$$

PWRatio =  $f(\text{Unitless}, \text{Length}, \text{Unitless}) \rightarrow \text{Unitless}$

[http://www1.eere.energy.gov/vehiclesandfuels/pdfs/basics/jtb\\_diesel\\_engine.pdf](http://www1.eere.energy.gov/vehiclesandfuels/pdfs/basics/jtb_diesel_engine.pdf)

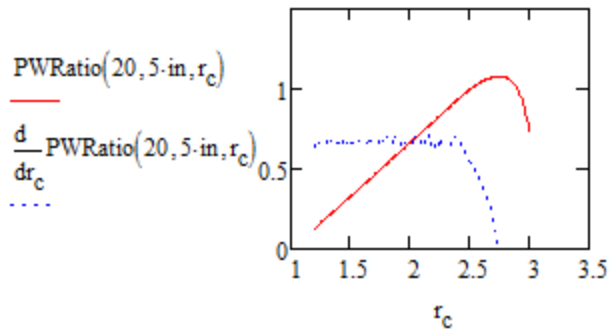
shows that the average efficiency for a diesel engine is 45%.

Increasing the compression ratio will increase the PW ratio until you reach the optimal compression ratio of 20.

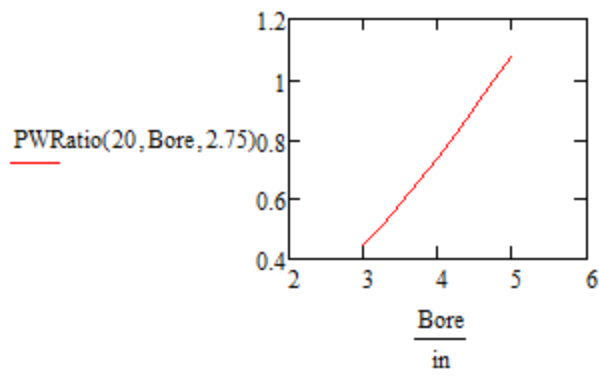


+

Increasing the cut-off ratio will increase the PW ratio until you reach the optimal cut-off ratio of 2.75



Increasing the bore will increase the PW ratio.



$$\text{PWRatio}(20, 5\text{in}, 2.75) = 1.079$$

+